

Heterogeneous Hydroformylation of Alkenes by Rh-based Catalysts

*Boyang Liu^a, Yu Wang^a, Ning Huang^{a, b}, Xiaocheng Lan^a, Zhenhua Xie^c, Jingguang G. Chen^{c, *},
Tiefeng Wang^{a, *}*

^a Beijing Key Laboratory of Green Reaction Engineering and Technology

Department of Chemical Engineering, Tsinghua University, Beijing 100084, China

^b Sinopec Economics and Development Research Institute Company Limited, Beijing 100029,
China

^c Department of Chemical Engineering, Columbia University, New York, NY 10027, USA

*Corresponding authors: Jingguang G. Chen (jgchen@columbia.edu); Tiefeng Wang
(wangtf@tsinghua.edu.cn)

Lead Contact: Tiefeng Wang (wangtf@tsinghua.edu.cn)

Summary:

Heterogeneously catalyzed hydroformylation reactions avert the problems of separation in homogeneous reactions, reduce the discharge of phosphorus-containing wastes, and prevent the loss of precious metals. This review summarizes recent developments of catalysts for heterogeneous hydroformylation in the last decade and proposes potential modification methods for future improvements. The hydroformylation properties of different reactants are compared to emphasize that various olefins face unique challenges. The hydroformylation of ethylene requires enhancement of catalytic activity and chemoselectivity, while that of propylene needs improvement in both chemoselectivity and regioselectivity. The hydroformylation of longer chain olefins and styrene seeks further improvement in regioselectivity. The catalytic properties of activity, selectivity and stability can be tuned through electronic effects (bimetallic effects, phosphine ligands, and single atom catalysts), steric hindrance (encapsulation structures, diphosphine ligands, and local functional groups), and reaction condition optimization (temperature, pressure, and solvents). The understanding of these effects is critical in future catalyst design for heterogeneous hydroformylation reactions.

Keywords: Heterogeneous hydroformylation, electronic effects, steric hindrance, reaction mechanism

1. Introduction

Hydroformylation reaction, which is one of the most important chemical reactions, produces more than 10 million tons of aldehydes per year.^{1,2} The reaction uses unsaturated olefins as reactants and the target products are functional aldehydes, which have potential applications in fragrance³ and pharmaceutical⁴ industries (**Scheme 1**). The possible side reactions are hydrogenation and isomerization, and the corresponding by-products are alkanes and internal olefins. The hydroformylation reaction is 100% atom economy (e.g., $\text{CH}_2=\text{CH}_2 + \text{CO} + \text{H}_2 \rightarrow \text{CH}_3\text{CH}_2\text{CH}=\text{O}$). The currently used homogeneous catalysts are highly active and selective.⁵⁻⁹ Through modification of the active center and ligands, researchers are able to tune the product composition, including chemoselectivity, regioselectivity, and enantioselectivity. Both electronic effects and steric hindrance were found to have significant impact on the catalytic activity and selectivity. However, homogeneous hydroformylation catalysts face severe separation challenges, which might cause precious metal leaching and phosphorus-containing waste discharge.¹⁰

The development of heterogeneous hydroformylation catalysts has attracted much attention in the last decade. Rh-based heterogeneous catalysts are mainly studied because the unmodified Rh metal is generally more active than any other metals.¹ Moreover, the other active metals, such as Co, Ir and Pd, typically require much higher reaction temperature and pressure for selective hydroformylation.^{5,11} Therefore, in this review we focus on Rh-based heterogeneous catalysts, which enable hydroformylation reactions under milder conditions.

The recyclability of heterogeneous catalysts overcomes the shortcomings of homogeneous counterparts, but introduces new challenges at the same time. Firstly, the activity of heterogeneous catalysts is generally much lower than that of homogeneous catalysts. Secondly, it

is difficult to tune the local environment for heterogeneous catalysts, which causes more challenges to the selectivity enhancement. In homogeneous catalysis, hydrogenation and isomerization products are rarely detected. However, by-products such as alkanes and internal olefins are formed in heterogeneous systems. Moreover, the reaction mechanisms of heterogeneous hydroformylation are not clear at present, leading to a lack of sufficient guidance for catalysts design. Although most of the homogeneous mechanism studies can be used as a reference, the heterogeneous systems have their own uniqueness, which requires far more investigations.

This review summarizes the research progress of heterogeneous hydroformylation catalysts in the last decade and attempts to bring forward some common practice in catalyst design. The hydroformylation performance of different catalysts is summarized for various reactants, because different olefin hydroformylation reactions face unique challenges. Typical reactants include ethylene, propylene, styrene and long chain terminal olefins. The reaction conditions of the first two are typically in gaseous environment, while the hydroformylation of the latter two are mostly carried out in solutions. As a consequence, the reaction temperature of ethylene and propylene hydroformylation is typically higher. Furthermore, only long chain terminal olefins are possible to isomerize to internal olefins. These differences lead to unique considerations in catalyst design and modification. Finally, we identify the trends of different heterogeneous hydroformylation catalysts and compare the differences of various reactants. Based on these results, we propose the main challenges for different alkenes and then provide guidance on potential optimization of catalytic performance.

2. Ethylene hydroformylation

Table 1 summarizes the ethylene hydroformylation results. The typical reaction temperature is 100-200 °C and the corresponding turnover frequency (TOF) is 10^1 - 10^3 h⁻¹. Ethylene hydroformylation is usually conducted in gaseous conditions and the main by-product is ethane. The only hydroformylation product is propionaldehyde, or with some 1-propanol if further hydrogenation of propionaldehyde occurs, free of regioselectivity or enantioselectivity issues. Therefore, the main challenges for ethylene hydroformylation are catalytic activity and chemoselectivity. The main competitive side reaction is the hydrogenation of ethylene to ethane.

Supported Rh catalysts showed a moderate activity and relatively low chemoselectivity (**Entries 1-2**).^{12,13} However, Shi et al.¹⁴ reported that unsupported Rh black showed a surprisingly high activity and aldehydes selectivity (**Entry 3**). The difference was possibly attributed to the introduction of solvents (toluene as solvent), where the concentration of reactants could be adjusted due to different solubility. The solvent effects, especially in the heterogeneous hydroformylation reactions, require more investigation. For the gaseous hydroformylation reactions, both the activity and chemoselectivity of pure Rh catalysts needed further improvements.

The addition of a secondary metal element to form a Rh-based bimetallic catalyst has been explored. Kunimori et al.¹⁵ compared the doping of V, Mo, Zn, and Fe, and found that Rh-VO₄ was the most active (**Entry 4**). Moreover, the addition of V enhanced the further hydrogenation of propionaldehyde to 1-propanol. The author proposed that highly dispersed Rh-VO₄ sites would produce more propanol and less ethane. More researchers tried Rh-Co bimetallic catalysts because Co was the second most active element for hydroformylation,¹ although its activity was much lower than that of Rh. Doping Co increased both the hydroformylation activity and oxygenates selectivity (**Entries 5-7**). X-ray absorption near edge structure (XANES)

measurements of Rh K-edge showed that surface Rh was more oxidized after Co doping,¹³ which was consistent with the *in situ* diffuse reflectance infrared Fourier transform spectroscopy (DRIFTS) results that the band position of adsorbed CO slightly blue-shifted on Rh-Co catalysts.¹⁷ Both XANES and DRIFTS results confirmed the electronic effects of Co doping, and density functional theory (DFT) calculations revealed the working mechanism. On the Rh(111) surface, the CO insertion was found to be rate determining (**Figure 1a**). Co doping decreased the activation energy from 0.91 to 0.85 eV, suggesting an enhanced hydroformylation activity. As for the selectivity enhancement, the adsorbed hydrogen atom competed against adsorbed CO for the same active site. The replacing energy of H substituting CO increased from 1.38 eV on Rh(111) to 1.49 eV on RhCo(111) surfaces, indicating that RhCo bimetallic catalysts should suppress the hydrogenation activity. The experimental measurements of the apparent activation energy (E_a) confirmed these trends that RhCo bimetallic catalysts had a smaller hydroformylation E_a and a larger hydrogenation E_a .¹⁷ Moreover, Christopher et al.¹⁸ synthesized ReO_x modified Rh single atom catalysts (SACs) on Al_2O_3 (**Entry 8**). Although the added Re existed in the oxidized form, the electronic effects of ReO_x were proven by the shifts in the CO stretching frequencies (**Figure 1b**) and shared some similarities to the bimetallic compounds. Further DFT calculations demonstrated that ReO_x withdrew electrons from the adjacent Rh atom and increased the hydroformylation activity by weakening CO adsorption.²⁴ The rate determining step (RDS) of ethylene hydroformylation changed from the CO insertion on $\text{Rh}/\text{Al}_2\text{O}_3$ to the coordination of the second CO on $\text{Rh}/2.9\text{ReO}_4\text{-Al}_2\text{O}_3$, leading to a lower activation energy and higher reaction rate.

In addition to the modification effect by secondary metal elements, organic phosphine ligands, which were proven to be effective in homogeneous systems, were directly applied in

heterogeneous catalysts as well (**Entries 9-12**). 3-Diphenylphosphinopropyltriethoxysilane (DPPPTS) was used to modify the SiO₂ surface and then Rh was loaded.¹⁹ The TOF of the as-synthesized catalysts increased by an order of magnitude compared to unmodified Rh catalysts, mainly due to the electronic effects of the phosphine ligands. Further coupling the bimetallic effects of Al enhanced the TOF to 134 h⁻¹ (**Entry 9**), which was attributed to the higher dispersion of Rh and a larger number of weak acid sites. Wang et al.²⁰ also tried to directly load the dpp* (PPh₂(CH₂)_nPPh₂) ligand on Rh/SiO₂ catalysts and found a significant enhancement of hydroformylation activity and chemoselectivity (**Entry 10**). The authors attributed the promotion to the electronic effects of phosphine ligands, which changed the RDS from the CO insertion to hydrogenation. Haumann et al.²¹ used supported ionic liquid phase (SILP) to immobilize homogeneous catalysts and obtained a relatively high chemoselectivity (**Entry 11**). Ding et al.²² functionalized the phosphine ligands and then polymerized them to porous organic ligands (POLs). The supported Rh existed as a quasi-homogeneous catalyst and exhibited a high hydroformylation activity (**Entry 12**). Since August 2020, the attempts to industrialization using Rh/POL-PPh₃ catalysts have been in progress, and the annual capacity reached 50,000 tons of propanol.²⁵

Inspired by the phosphine ligands, Schunk et al.^{23,26} used platinum group metal inorganic phosphides to catalyze ethylene hydroformylation reactions and obtained 80% chemoselectivity (**Entry 13**). The reaction conditions also significantly influenced the chemoselectivity, with lower temperature and higher CO content favoring the formation of aldehydes. The addition of water further increased the selectivity to aldehydes, which was possibly attributed to selective blocking of the hydrogenation sites.

Figure 2 summarizes the catalytic performance of the catalysts mentioned above. A general trend regarding chemoselectivity and modification strategies for Rh active sites can be found: organic phosphines > inorganic phosphorus > secondary metal > bulk Rh. The only exception was the Rh black catalyst where the solvent was introduced in the reaction. The electronic environment around the Rh sites influenced the activation energy and even changed the RDS of the surface reaction. The RDS of ethylene hydroformylation on Rh was CO insertion and its energy barrier was much higher than other steps.¹⁷ Therefore, the major obstacle to chemoselectivity was the sluggish CO insertion process. The addition of a secondary metal element decreased the activation energy of CO insertion, which slightly increased the chemoselectivity. The phosphine ligands further reduced this activation energy, and even changed the RDS to other hydrogenation steps. Therefore, these phosphine-modified catalysts showed a high chemoselectivity of > 95%. In conclusion, the major challenge for heterogeneous hydroformylation of ethylene is the enhancement of chemoselectivity to aldehydes against hydrogenation side products, and the primary strategy is to reduce the activation energy of CO insertion.

3. Propylene hydroformylation

Similar to ethylene hydroformylation, propylene hydroformylation reactions are usually conducted in gas phase and the main products are butyraldehyde and propane. However, due to the asymmetry of propylene, the regioselectivity also becomes a criterion to judge the catalyst performance. The molar ratio (*l/b*) of linear to branched aldehydes is usually chosen to evaluate the regioselectivity. In this section, the value of *l/b* is defined as the ratio of n-butanal to iso-

butanal. **Table 2** summarizes the reaction data of propylene hydroformylation on different heterogeneous catalysts.

The unmodified Rh/SiO₂ was chosen as the reference sample, which had a relatively low hydroformylation activity and chemoselectivity (**Entry 1**). However, the *l/b* ratio was 2.23,²⁷ indicating that linear products were preferred. Similar to ethylene hydroformylation, secondary metal modification has also attracted much attention. Kunimori et al.^{28,29} used transition metal doping to enhance the hydroformylation activity, chemoselectivity and regioselectivity (**Entries 2-3**). Sordelli et al.²⁷ compared the modification effect of the alkali metals and reported an activity promotion trend of Li > Na > K > Rb >> Cs (**Entry 4**). The authors attributed this trend to the positive impacts of stronger polarizing capability and more acidic surfaces. A similar trend of Li > Na > K was also observed in vinyl acetate hydroformylation, while the modification of the alkali-earth cations followed the trend of Mg > Sr > Ca.³⁶ These electronic effects played an important role on activity but showed little influence on regioselectivity. However, Li et al.³⁰ synthesized K-promoted Rh clusters encapsulated in silicate-1 zeolite, which showed significantly higher activity, chemoselectivity and regioselectivity (**Entry 5**). Compared to previously reported Rh-K/SiO₂ catalysts,²⁷ the TOF increased by 4 orders of magnitude, which could hardly be explained by the effect of reaction temperature and pressure. Interestingly, the relatively high activity of the K₂₀[^]Rh@S-1 catalyst was also obtained in toluene, similar to the Rh-black catalysts in ethylene hydroformylation (**Table 1 Entry 3**). Although the introduction of solvent might be responsible, more systematic studies of solvent effects would be needed. In addition to the activity enhancement, K modification also exhibited steric hindrance, which restricted the adsorption configuration of propylene and increased the regioselectivity to linear aldehydes (**Figure 3a**). An optimized K/Rh ratio was discovered, because insufficient K would

result in a lack of steric hindrance and no regioselectivity, while redundant K would block the active sites and suppress reactivity.

Apart from metal modification, phosphine ligands are effective in promoting propylene hydroformylation reactions. Traditional triphenylphosphine (PPh₃) ligands enhanced the hydroformylation activity through electronic effects, while bidentate Xantphos further regulated the regioselectivity through steric hindrance. A simple co-impregnation strategy increased the *l/b* ratio to 15 on Rh-Xantphos/SiO₂ (**Entry 6**).³¹ Using SILP further increased the TOF, but sacrificed part of the regioselectivity (**Entry 7**).³² Both electronic effects and steric hindrance affected the regioselectivity. By tuning the functional group of PPh₃ ligands, Bell et al.³¹ reported that the *l/b* ratio increased with decreasing electron density around Rh. Simultaneously, a greater degree of steric hindrance favored the formation of linear products. Moreover, the activation energy for n-butanal was lower than that for iso-butanal on Rh-Xantphos/SiO₂ catalysts, causing a decrease in the *l/b* ratio with increasing temperature (**Figure 3b**). Ding et al.³³ co-polymerized vinyl biphephos and tris(4-vinphenyl)phosphane, and supported atomically dispersed Rh atoms on these POLs (**Entry 8**). The obtained high activity was attributed to highly exposed surface phosphorus and single atom Rh sites, while the high regioselectivity was ascribed to the high steric hindrance of biphephos in the copolymer skeleton. The feasibility is currently being tested for commercial processes. Shi et al.³⁴ copolymerized 4,4',4''-phosphanetriyltribenzaldehyde (PTBA) with hydrazine (HA) to form porous organic polymers (POPs), which was similar to POLs. The surface Rh atoms were atomically dispersed and a high *l/b* ratio was also obtained (**Entry 9**).

Furthermore, SACs supported on inorganic supports were also studied and the catalytic performance was outstanding. The TOF reached >2000 h⁻¹ on Rh₁/CoO, while the *l/b* ratio was

15 (**Entry 10**). SACs were considered as the bridge between heterogeneous and homogeneous catalysis,^{37,38} and DFT calculations showed that atomically dispersed surface Rh atoms were similar to homogeneous sites. The activation energy to linear aldehydes was 0.06 eV smaller than that to branched products, which was similar to the results of Rh-Xantphos/SiO₂ catalysts.³²

The propylene hydroformylation results are summarized in **Figure 4**. The chemoselectivity followed the trend of secondary metal modification < phosphine doping, which was the same as that of ethylene hydroformylation. Interestingly, two exceptions (K₂₀⁺Rh@S-1 and Rh₁/CoO) were observed, where solvent was introduced during the reaction. Similar to the reported high chemoselectivity of Rh-black in ethylene hydroformylation, the existence of proper solvent might also increase the chemoselectivity of hydroformylation of propylene.

Controlling the regioselectivity is a critical issue in propylene hydroformylation. The approach to increasing the *l/b* ratio includes electronic adjustment (ligands, SACs), steric hindrance (chelate ligands, alkali metals), and reaction condition optimization. The effects of changing reaction conditions were highly related to the catalyst properties. **Figure 5** compared the *l/b* ratio as a function of TOF. The target areas of catalysts design were the top right and bottom right regions, corresponding to linear selective and branched selective catalysts with a high activity, respectively. All the above catalysts showed a *l/b* ratio >1, indicating that the production of n-butanal was favorable. The current studies focused on increasing the linear selectivity and the enveloping line was plotted by a dashed line. The current selectivity has met the demands of industrial use, and further breakthrough should focus on enhancing the stability, increasing the atomic efficiency and reducing the cost of catalyst synthesis.

4. Longer chain linear α -olefin hydroformylation

Fatty aldehydes have many applications and can be produced from α -olefins through hydroformylation reactions. This section focuses on olefins containing longer carbon-carbon chains, such as 1-hexene and 1-octene. Their chemical properties and reaction pathways are very similar and thus are discussed together in this section. Due to their relatively long carbon chain, these olefins are in liquid phase during reactions and most researchers use toluene as the solvent. Relatively high pressures of H_2 and CO are used to enhance the gas-liquid mass transfer rate, and a relatively high chemoselectivity is obtained. However, the long chain olefins might undergo C=C isomerization reactions, which have not been discussed for the other reactants. Therefore, the main side reaction for α -olefins ($>C_4$) hydroformylation is isomerization and the corresponding by-products are internal olefins, which can further undergo hydroformylation reactions to form branched aldehydes at different positions. In summary, one needs to consider hydroformylation, hydrogenation and isomerization reactions for α -olefins, and the products contain linear aldehydes, branched aldehydes, alkanes and internal olefins.

Table 3 summarizes the catalysts used in 1-hexene hydroformylation reactions. The reaction temperature was generally lower than that of ethylene and propylene hydroformylation, typically at ≤ 120 °C. The pressure of syngas ranged from 1 to 7 MPa, and mostly at 4–5 MPa. The chemoselectivity was typically $>90\%$, indicating that the hydrogenation products could usually be neglected.

The catalytic performance of simple Rh sites differed from each other on different supports (**Entries 1-6**). Haukka et al.⁴⁰ compared different metal oxide supports and proposed that nano-supports were more active than normal counterparts (**Entries 2-3**). A larger surface area and higher amount of weak acid sites enhanced the catalytic activity. Tsubaki et al.⁴² compared different carbon supports and reported an activity trend of reduced graphene oxide (RGO) >

carbon nanotubes (CNTs) > active carbon (AC) (**Entry 5**). The larger exposed surface area and higher Rh dispersion contributed to the higher activity of Rh/RGO.⁴² Using HNO₃ solution to treat AC introduced surface functional groups and further restricted the adsorption geometry of 1-hexene, leading to a higher *l/b* ratio (**Entry 6, Figure 6a**).⁴³ These results implied that the properties of supports significantly influenced the catalytic performance of surface Rh, through both electronic effects and steric hindrance.

In addition to changing the supports, researchers also tried encapsulating the active sites by zeolites or MOFs. The encapsulation structure could not only provide some steric hindrance to increase the regioselectivity, but also enhance the stability and suppress Rh leaching. Tsubaki et al.⁴⁴ used silicalite-1 to enfold the Rh/AC catalysts (**Entry 7**) and obtained a similar *l/b* ratio to that with the HNO₃-treated ones (**Entry 6**). Li et al.⁴⁵ reported a Rh@ZIF-8 catalyst, which however rarely showed regioselectivity (**Entry 8**). Schulz et al.⁴⁶ used MOF-5 as the enclosure material and the low conversion of cyclohexene confirmed the encapsulation structure. The Rh/MOF-5 catalyst showed a higher TOF of >9000 h⁻¹ in 1-hexene hydroformylation with a good regioselectivity, but the yield to aldehydes was relatively low (**Entry 9**). Changing the shell material to MIL-101 could further enhance the activity (**Entry 10**).⁴⁷ The steric hindrance of the cages in MOFs limited the access of internal olefins, which increased the *l/b* ratio (**Figure 6b**). Zhang et al.⁴⁹ encapsulated Rh₂O₃ in microporous silicalite-1, but showed no regioselectivity for 1-hexene hydroformylation (**Entry 12**). Interestingly, increasing the carbon chain of the reactants increased the selectivity to linear aldehydes. The *l/b* ratio of 1-octene and 1-dodecene hydroformylation increased to 1.71 and 2.46, respectively (**Table 4 Entry 2**). This was because longer olefins were more sterically hindered and the corresponding branched aldehydes diffuse through the microchannels of the zeolite with a larger resistance. Therefore, the pore size of the

shell needed to match the size of reactant molecules for the best regioselectivity performance. This was the possible explanation for the absence of regioselectivity for Rh@ZIF-8 catalysts (**Entry 8**).

The third modification method was to dope inorganic additives. The bimetallic Rh-Co layered hydrotalcite-type catalyst, RhCoHT-1, was highly selective to linear aldehydes in 1-hexene hydroformylation (**Entry 13**), but highly selective to branched aldehydes in 1-octene hydroformylation (**Table 4 Entry 4**), the underlying mechanism of which required more investigations. Li et al.³⁰ also used the K⁺Rh@S-1 catalysts in 1-hexene hydroformylation. Different from propylene hydroformylation (**Table 2 Entry 5**), the optimized K doping amount was relatively low (**Entry 14**). Due to the larger size of 1-hexene, a smaller amount of K could provide sufficient steric hindrance to increase the regioselectivity to linear aldehydes.

The fourth modification strategy was to load organic phosphine ligands on Rh catalysts or use phosphine ligands to fix Rh metals. The addition of PPh₃ to both SiO₂ and RGO supported Rh catalysts showed an increased TOF and *l/b* ratio (**Entries 15–16**). The coordination of PPh₃ tuned the electronic structure of surface Rh atoms and then influenced the adsorption state of reactants.⁵¹ Moreover, PPh₃ could provide some steric hindrance, which further increased the regioselectivity to linear aldehydes.⁵² Instead of using Rh to fix phosphine, Jasra et al.⁵⁴ first loaded tris(3-sodium sulfonatophenyl) phosphine (TPPTS) on hydrotalcite and used Rh-P coordination to fix Rh. However, due to the strong interaction, TPPTS was restricted in hydrotalcite and the steric effects of ligand were not significant.⁵⁴ As a result, the products showed basically no regioselectivity (**Entry 18**). The addition of diphosphine monomers to POLs or POPs significantly increased the regioselectivity (**Entries 19–21**). Ding et al.^{55,62} found that without the assistance of phosphine ligands, simple Rh catalysts converted most of the

reactants to alkanes and iso-alkenes, indicating that hydrogenation and isomerization were dominant. On the contrary, the Xantphos-doped Rh/POPs-PPh₃ catalysts showed good performance in hydroformylation activity and regioselectivity (**Entry 19**). The PPh₃ monomers mainly contributed to the activity promotion through electronic effects, while the Xantphos ligands enhanced the regioselectivity by steric hindrance (**Figure 6c**).⁵⁵ Changing the diphosphine ligand from Xantphos to bisphosphoramidite (BPa) further increased the *l/b* ratio to 34 (**Entry 20**), which was attributed to the synergetic effects of PPh₃ and BPa moieties.⁵⁶ Changing the PPh₃ monomer to vinylbenzene (VB) further increased the selectivity to linear aldehydes (**Entry 21**).⁵⁷ Shi et al.³⁴ used monophosphine (PTBA) and hydrazine (HA) as the monomer to encapsulate Rh and obtained a high regioselectivity (**Entry 22**). The molecular size of amine linkers affected the steric hindrance, which in turn affected the regioselectivity. Smaller amine linker favored the formation of linear aldehydes. However, the chain length of linear olefins showed no relationship with regioselectivity, indicating that the steric hindrance originated from the pore structure. Comparing the results of **Entries 19-22**, one could further subdivide the steric hindrance into two types: the long-range hindrance and short-range hindrance (**Scheme 2**). The former usually originated from the pore structure and could be tuned by changing the encapsulation material. MOFs, zeolite and POPs shells with specific pore size might tune the regioselectivity through long-range hindrance, possibly by varying the diffusion properties of the reactants and products. Varying the pore size could significantly influence the product distribution (like changing the amine linkers in **Entry 22**). Moreover, Ranocchiari et al.⁶³ considered the MOF encapsulation as a kinetic modulator in Co-based catalysts, and discovered that the MOF-confinement changed the local concentration of reactants and products in micropores, which further increased the branched selectivity. The short-range hindrance was

the local environment around Rh active sites, and could be modified by ligands or other additives. In the Rh/POL-PPh₃ type catalysts, changing the position of vinyl groups in PPh₃ monomers affected the catalytic performance.⁶⁶ The m-POL-PPh₃ catalyst was preferred because of the relative ease to form the HRh(CO)₂(PPh₃-POL)₂ species due to the favorable microenvironment. Similarly, the replacement of diphosphine ligands influenced the short-range hindrance (**Entries 19-21**). The addition of K (**Entry 14**) and the modification of HNO₃ (**Entry 6**) could also be classified as the short-range hindrance, which usually functioned by controlling the adsorption geometry of reactants.

The fifth modification strategy was to use SACs. In well-structured Rh₂P catalysts, surface Rh atoms were all separated by inorganic phosphorus and thus Rh-based phosphides could be considered as a special type of SACs, according to the definition of Zhang et al.⁶¹ The supported Rh₂P@C showed a relatively high TOF of 5727 h⁻¹ in 1-hexene hydroformylation reactions (**Entry 23**).⁵⁸ However, typically no regioselectivity was observed, which was attributed to the lack of steric hindrance.

Table 4 summarizes the catalytic performance in 1-octene hydroformylation reactions. Because the properties of 1-hexene and 1-octene were very similar, the catalyst design strategies are basically the same. Many literatures also evaluate the same catalysts in hydroformylation reactions of both reactants. Therefore, in the following part we only discuss the new catalysts that have not been mentioned above. Similar to 1-hexene hydroformylation, the 1-octene hydroformylation produces alkanes, iso-alkenes, linear and branched aldehydes, which correspond to the hydrogenation, isomerization and hydroformylation products, respectively.

The porous covalent triazine frameworks (CTFs) were used as the encapsulation material of Rh catalysts, which led to a better recyclability (**Entry 3**).⁶⁴ The concept of CTFs encapsulation was basically the same as MOFs and silicate encapsulation, with only minor differences in the shell materials and synthesis methods. The TPPTS ligands were also fixed in MCM-41, and the Rh-TPPTS@MCM-41 catalysts⁶⁵ showed a higher *l/b* ratio than hydrotalcite encapsulated counterparts, possibly due to the suitable pore size (**Entries 8-9**). Moreover, researchers proposed that nitrogen had some similarities to phosphine ligands.⁷⁰ Rosenberg and Karakhanov et al.^{59,67} anchored Rh sites on polyamine modified silica surfaces (**Figure 6d**, **Entries 10-11**). The authors proposed that Rh complex leached into the liquid phase under reaction conditions and catalyzed the reaction in a homogeneous form. After cooling to room temperature and removing the CO atmosphere, Rh was then recaptured by the surface amine groups,⁵⁹ similar to an earlier report of the release-and-catch mechanism by Gascon et al.⁶⁹ in Rh-PTA@MIL-101. Further changing the surface functional groups, the aldehydes were hydrogenated to alcohols in a tandem reaction.⁶⁷ Ding et al.⁶⁸ reported that Rh/POL-PPh₃ catalysts showed enhanced activity in comparison to homogeneous catalysts like RhH(CO)(PPh₃)₃ (**Entry 13**), due to the high concentration of flexible PPh₃. However, this catalyst showed no regioselectivity. This result was an addition to the previous conclusion that PPh₃ monomer contributed to the activity promotion, while the Xantphos ligands enhanced the regioselectivity on the Rh-Xantphos/POPs-PPh₃ catalysts (**Table 3 Entry 19**). Xiao et al.⁶⁰ used cationic template and anionic ligand to synthesize porous supramolecular assemblies (PSAs), which interacted with Rh metals by Rh-P coordination (**Figure 6e**). Without the addition of phosphine moieties, the Rh/TPPTS [Trisodium 3,3',3''-phosphanetriyltri(benzene-1-sulfonate)] catalyst showed a very low aldehydes selectivity (31.2%) with the other products being iso-alkenes similar to the Rh(CO)₂(acac) catalyst.⁵⁵ The

addition of PPh₃ moieties significantly increased the aldehyde selectivity to 98.4%. However, the *l/b* ratio was 2.8, implying a slight selectivity to linear aldehydes. The replacement of PPh₃ to Xantphos moieties further increased the *l/b* ratio to 39 (**Entry 18**), demonstrating that the short-range steric hindrance significantly influenced the regioselectivity. Apart from the modification of organic phosphines and inorganic phosphides, inorganic phosphates were also used in hydroformylation reactions. Gascon et al.⁶⁹ synthesized immobilized Rh complex in phosphotungstic acid (PTA)-MIL-101(Cr) composites, and obtained a better stability, but the activity and regioselectivity were not enhanced.

Some longer chain olefins were also used as reactants. Sun et al.⁷⁷ prepared Rh-Co-Pi/ZnO catalysts where Rh was atomically dispersed, and used them in 1-decene hydroformylation reactions. The addition of phosphorus increased the dispersion and Co withdrew electrons from Rh. The electronic structure modification adjusted the adsorption mode of alkene, which was proved by *in situ* DRIFTS, and thus increased the *l/b* ratio from 0.7 on Rh/ZnO to 2.1 on Rh-Co-Pi/ZnO. Wei et al.⁷⁸ encapsulated the Rh/ZnO catalyst by ZIF-8 and evaluated its catalytic performance in 1-dodecene hydroformylation. The encapsulation structure had no influence on regioselectivity, but showed better stability and recyclability.

Figure 7 summarizes the 1-hexene and 1-octene hydroformylation performance, and the envelope curves are plotted by dashed lines. Generally, most data points are located above the line of *l/b*=1, indicating that linear α -olefins are easier to be converted to linear aldehydes. This result is similar to propylene hydroformylation. The highest linear aldehyde selectivity exceeds 95%, and a high *l/b* ratio is only obtained on catalysts with phosphine ligands. Further development of highly selective catalysts without the addition of phosphine requires more investigations.

5. Styrene hydroformylation

Besides linear olefins, aromatic olefins are also used as reactants in hydroformylation reactions. Due to the highly conjugated structure of styrene, isomerization reaction cannot occur. Therefore, the main by-products of styrene hydroformylation are ethylbenzene from the undesired hydrogenation. The linear and branched hydroformylation products are 3-phenylpropionaldehyde and 2-phenylpropionaldehyde, respectively. Moreover, the 2-phenylpropionaldehyde has chiral isomerism, leading to considerations of chemoselectivity, regioselectivity and enantioselectivity.

Table 5 summarizes the catalytic performance of styrene hydroformylation reactions. Due to the high boiling temperature of styrene, all hydroformylation reactions were conducted in liquid phase and most researchers used toluene as the solvent. Moreover, the overall chemoselectivity was usually above 95%, which was higher than that of gaseous ethylene and propylene hydroformylation. Therefore, the concentration of hydrogenation products could be ignored and the main challenge of styrene hydroformylation was the enhancement of activity and regioselectivity.

The supported and unsupported Rh catalysts were chosen as the reference samples (**Entries 1-3**), which had a low TOF. Usually, unmodified catalysts such as Rh-black did not show regioselectivity (**Entry 3**), while supported Rh catalysts on Al₂O₃ were slightly selective to branched aldehydes (**Entry 2**). The difference of regioselectivity was possibly attributed to the different reaction conditions that high pressure of syngas and low reaction temperature favored the formation of 2-phenylpropionaldehyde.⁸⁰ However, this catalyst had the problem of severe Rh leaching under the reaction conditions of high pressure. Huang et al.⁸¹⁻⁸³ doped B and S on TiO₂ and g-C₃N₄ and used them as supports, the TOF of which was significantly enhanced

(Entries 4-6). In comparison to unmodified Rh catalysts supported on the same supports, the TOF increased twice due to modification of the delocalized conjugated π structure. However, regioselectivity was not affected.

Organic phosphine ligands were also introduced to improve the catalytic performance. The first method was to directly co-impregnate Rh with phosphine ligands. The addition of PPh_3 slightly increased the TOF, but significantly increased the selectivity to 2-phenylpropionaldehyde (**Entries 1 and 7**). Abdi et al.⁵³ directly loaded $\text{HRh}(\text{CO})(\text{PPh}_3)_3$ active sites on active carbon synthesized from mango seeds, and obtained a TOF of 294 h^{-1} with a *l/b* ratio of 0.30 (**Entry 8**). In addition to the above ligands, chiral ligands were also used to realize enantioselectivity. The doping of BINAP decreased the TOF to $\sim 20 \text{ h}^{-1}$, which was lower than that of PPh_3 modified catalysts (**Entries 9-10**). However, the regioselectivity was essentially unchanged and the production of branched aldehydes was also preferred. The products showed some enantioselectivity due to the chiral ligands and the enantiomeric excess (ee) value reached $\sim 30\%$ on the Rh-BINAP(R)/ SiO_2 catalysts. The second method of phosphine addition was to decorate the support surface by functional groups and then fix Rh atoms using the coordination effect. Fe_3O_4 with surface decoration was used to enhance the separation through magnetism (**Entries 11-13**). Firstly, the amino ligands were decorated on silica, which wrapped the Fe_3O_4 core. Surface Rh atoms were then fixed by the amino groups, but the TOF was very low at 12.5 h^{-1} (**Entry 11**). Further changing the amino group to phosphine ligands slightly increased the TOF with some sacrifice of branched aldehydes selectivity (**Entry 12**). The application of ferrocenylphosphine increased the linear selectivity to 51.9%, while the TOF was still lower than unmodified supported Rh catalysts (**Entry 13, Figure 8a**). The third method was to directly use the phosphine ligands as catalyst supports. Smith et al.⁷³ loaded Rh on metallodendrimers (**Entry**

14). Both activity and regioselectivity were tuned by carefully modifying the ligand structure. The branched aldehyde selectivity reached 88% at a TOF of 100 h⁻¹. Fan et al.⁸⁷ synthesized phosphine-based functional covalent organic frameworks (COFs) to fix Rh atoms (**Entry 15**). The TOF reached 2557 h⁻¹, but no regioselectivity was observed. Xiao et al.^{74,88} and Ding et al.^{76,89} added functional groups on phosphine ligands and then polymerized them as the supports (**Entries 16-20**). With increasing amount of PPh₃ moieties, the pore volume increased and the catalytic activity, chemoselectivity and regioselectivity to 2-phenylpropionaldehyde all increased (**Entry 16**).⁸⁸ The authors attributed the enhanced performance to the existence of excess free phosphine ligands. The high concentration and mobility of 2-bis(diphenylphosphino)ethane (dppe) ligands in the POL frameworks were found to be important for catalytic performance as well (**Entry 17**).⁷⁴ Xiao et al.⁷⁴ also reported that low reaction temperature and high pressure favored the formation of branched aldehydes. The *l/b* ratio decreased from 0.38 to 0.05 when decreasing the reaction temperature from 110 to 50 °C. This result indicated that the optimization of reaction conditions was important to tune the regioselectivity. Ding et al.⁷⁶ synthesized PPh₃-derived porous organic cages (POCs) to support Rh and obtained a relatively high linear aldehydes selectivity (**Entry 18**). The dual P coordination gave a higher linear regioselectivity due to favorable electron and steric structures (**Figure 8b**). A weaker σ -donor and a better π -acceptor were preferred, and a larger steric hindrance was achieved on dual P coordinated catalysts. Using chiral diphosphine monomers to synthesize POL supports increased the regioselectivity to branched aldehydes and showed product enantioselectivity (**Entry 20**). The highest ee value reached 58.9%,⁸⁹ which was higher than that over the Rh-BINAP(R)/SiO₂ catalyst.

Different inorganic supports were used to tune the local environment of surface Rh single atoms and the catalytic performance was thus enhanced. Zhang et al.⁹⁰ first reported atomically dispersed Rh on ZnO nanowires and obtained a TOF of $>3000 \text{ h}^{-1}$ (**Entry 21**), although no regioselectivity was observed and the loading amount of Rh was relatively low. Changing the support to CeO₂ significantly decreased the activity (**Entry 22**), but enabled the catalyst to produce in situ hydrogen from a low-temperature water gas shift (WGS) reaction. The *l/b* ratio was then enhanced to ~ 3 when using CO and H₂O as the reactants (**Figure 8c**).⁹¹ Plessow et al.⁹² calculated the stability of Rh single atoms on different oxide surfaces and discovered that Rh₁/MgO was the most stable one but showed no hydroformylation reactivity. The strong interaction between Rh and MgO limited the flexibility of the catalysts, which reduced the activity. On the contrary, Rh₁/CeO₂ was not very stable and showed a good catalytic activity (**Entry 23**). The recyclability test of Rh₁/CeO₂ showed an obvious decline in activity after one run, which was attributed to the leaching of Rh.⁹¹ Yan et al.⁹³ used ionic liquid (IL) to stabilize surface Rh atoms on Rh₁/TiO₂ catalysts (**Entry 24**) the structure of which was confirmed by high-angle annular dark-field scanning transmission electron microscopy (HAADF-STEM), extended X-ray absorption fine structure (EXAFS) and Fourier transform infrared spectroscopy (FTIR) measurements (**Figure 8e**). Although the TOF decreased by 30% in comparison with IL-free catalysts, the stability was significantly enhanced, and the IL-induced catalyst had a higher TOF than the IL-free one since the second run. The IL was believed to act as a linker to bind the active sites and the TiO₂ support and suppressed Rh leaching. Researchers also tried other modification strategies to further tune the regioselectivity. Agnoli et al.⁹⁴ loaded Rh₁ on Mn-based metal-organic frameworks (MOFs) and obtained a higher 2-phenylpropionaldehyde selectivity of 72.5% (**Entry 25**) by combining the modification of encapsulation structure and

the unique electronic environment around Rh single atoms. Chen and Liang et al.⁴ used phosphorus coordinated Rh₁ supported on nanodiamond (ND), and obtained a *l/b* ratio of 0.08 at a TOF of 95 h⁻¹ (**Entry 26, Figure 8d**), which was better than any other counterparts. This enhanced regioselectivity was attributed to the high electron density of Rh atoms, where Rh^{δ+} and the large angle between *gem*-dicarbonyl Rh(CO)₂ favored branched aldehydes. This catalyst was used in the synthesis of pharmaceutical molecules Ibuprofen and Fendiline, which also showed good regioselectivity. As discussed in section 4, Rh₂P can also be considered as a special type of SACs. Wang et al.⁹⁵ used PPh₃ as the phosphorus source to synthesize inorganic phosphides Rh₂P at a relatively low temperature. The TOF reached ~1500 h⁻¹, which was attributed to both geometric and electronic effects (**Entry 27**). The surface Rh atoms were separated by P, and electrons transferred from Rh to P, resulting in positively charged surface Rh sites. The doping of secondary metal to Rh₂P further promoted the activity due to an optimized electronic structure (**Entry 28**).^{17,96} The addition of Co did not change the structure of metal phosphides, which remained similar to Rh₂P, as shown by the X-ray diffraction (XRD) patterns (**Figure 8f**). The only difference was that Co addition decreased the lattice constant, due to the smaller covalent radius of Co in comparison to that of Rh. Through the modification of the electronic structure around Rh sites, Co addition destabilized hydrogen adsorption and decreased the activation energy of the RDS simultaneously. Thus, the activity showed a volcanic relationship against the Co amount. Comparing these catalytic results of SACs (**Entries 21-28**), only Rh₁/Mn-MOF (**Entry 25**) and Rh₁/PNP-ND (**Entry 26**) showed regioselectivity to branched aldehydes, likely originated from the steric hindrance of either MOFs shell or local phosphorus ligands.

To briefly summarize, both the electronic effects and steric hindrance affect styrene hydroformylation. The electronic structure can be regulated by adding secondary elements, fixing phosphine ligands, changing supports to synthesize SACs, and doping inorganic phosphorus. These modifications not only enhance the catalytic activity, but also show some influences on the regioselectivity. The steric hindrance mainly comes from diphosphine ligands, which do not increase the reactivity but show a significant impact on the product distribution. By tuning the ligand structure and P coordination environment, both regioselectivity and enantioselectivity can be modified. Moreover, the reaction conditions also affect the regioselectivity. Low temperature favors the formation of branched aldehydes,^{74,92} which is contrary to the conclusion of propylene hydroformylation.³¹ Moreover, a higher syngas pressure favored the formation of branched aldehydes in styrene hydroformylation on rhodium phosphides.⁹⁷ Through the optimization of reaction conditions, a high regioselectivity of branched aldehydes (>95%) could be obtained (**Entry 29**). The solvent polarity also plays an important role in regioselectivity, and a less polar solvent favors the formation of 2-phenylpropionaldehyde.^{85,86}

Figure 9 summarizes the catalytic performance of the above catalysts. Most data points are located in the lower half of the graph, indicating that styrene hydroformylation tends to produce branched aldehydes with the highest reported *l/b* ratio being ~1.3, which is contrary to propylene and other linear α -olefin hydroformylation. This phenomenon is possibly attributed to the formation of stable Rh-benzylic intermediates, which favor the generation of 2-phenylpropionaldehyde.^{34,98} On the contrary, the selectivity to branched products can reach >95%, but the regioselectivity decreases with increasing TOF. The enveloping line is plotted in **Figure 9**, and future challenges are how to break this limit. There has been some

progress in the improvement of linear selectivity. However, the relatively high *l/b* ratio could only be obtained with homogeneous catalysts, using specially designed phosphine ligands.^{105,106} It still remains challenging to obtain a high linear regioselectivity for heterogeneous hydroformylation of styrene.

6. Effect of hydroformylation reaction conditions

In addition to catalyst structure design, the variation of reaction conditions also influenced the regioselectivity (**Figure 10**). The first variable was the reaction temperature. Many researchers^{41,42,49,57} believed that high temperature decreased the *l/b* ratio in linear olefins hydroformylation because more isomerization reactions occurred at high temperatures (**Figure 10a**). This conclusion was similar to propylene hydroformylation,³¹ but different from styrene hydroformylation.^{74,92} One possible explanation was that high temperature promoted the isomerization reactions, and the isomerized internal olefins would further undergo hydroformylation reactions to produce branched aldehydes and decrease the *l/b* ratio. Styrene, however, could not be isomerized, and thus the high temperature would not decrease the *l/b* ratio. Moreover, some catalysts, like Rh-Xantphos/POPs-PPh₃⁵⁵ and RhCoHT-1,⁵⁰ showed no relationship between regioselectivity and reaction temperature in 1-octene hydroformylation reactions. The cause of this phenomenon was possibly attributed to the unique catalyst structure, which required further investigations.

The second variable was the pressure of syngas (**Figure 10b**). Some catalysts, like Rh-Xantphos/POPs-PPh₃⁵⁵ and Rh/Cu₂O,⁴¹ showed a negative relationship between total pressure and *l/b* ratio in linear α -olefins hydroformylation. On the contrary, the *l/b* ratio increased with syngas pressure on the RhCoHT-1 catalyst.⁵⁰ The Rh/CPOL-BPa&1VB catalyst⁵⁷ showed a

volcanic relationship with the syngas pressure, and the highest linear selectivity was obtained at 2 MPa. The above results demonstrated that the reaction conditions for different catalysts needed to be optimized separately, and the optimized temperature and pressure were strongly correlated to the catalyst properties and surface reaction mechanism.

The third variable was the solvent. Bhanage et al.⁴¹ compared different solvents and found that toluene provided the highest selectivity to aldehydes in 1-hexene hydroformylation, but the *l/b* ratio in toluene was the lowest. In a homogeneous system, the solubility of H₂ and CO was very important for the solvent effect on Rh-phosphine catalysts,^{99,100} while the mechanism of solvent effects for heterogeneous catalysts required more studies.

7. Challenges for hydroformylation of different reactants

We have discussed the hydroformylation reactions of different olefins on various catalysts. In this section, we organize the above data and aim to propose the unique challenges and corresponding solutions for different olefin reactants, based on the understanding of structure-performance relationship. **Table 6** summarizes the existing challenges for different reactants and the influence of potential solutions. The chemoselectivity is significant for ethylene and propylene hydroformylation, while regioselectivity is important for propylene, linear α -olefin and styrene hydroformylation. Regarding the structure-performance relationship, the modification of electronic structure should significantly influence the catalytic activity and chemoselectivity, with less impact on the regioselectivity. The steric hindrance, on the contrary, has little effect on the activity and chemoselectivity, but is significant for the regioselectivity. Moreover, the reaction conditions would also influence the regioselectivity.

Firstly, we would like to focus on the hydroformylation activity. Considering that the TOF is strongly dependent on the reaction temperature, simply comparing the values of TOF is not meaningful. However, we could draw some conclusions based on the mechanism studies. DFT calculations revealed that on pure Rh catalysts, the CO insertion was the RDS and limited the catalytic activity,^{17,24,95} which was confirmed by the kinetic order and experimental data.^{12,18} Therefore, an efficient approach to increasing the activity was to decrease the activation energy of CO insertion. Due to the relatively small size of CO, the steric hindrance could hardly affect the CO adsorption and diffusion on catalyst surface. Thus, electronic effects were the most efficient way for activity promotion. By adding suitable additives or synthesizing SACs, the electronic structure of Rh sites could be tuned and the CO insertion would be accelerated,¹⁷ even resulting in a change of the RDS to acyl hydrogenation^{20,35,95} or CO co-adsorption.²⁴ Very recently, Mao et al.¹⁰¹ compared the reaction mechanism of ethylene and propylene hydroformylation reactions on the same RhCo₃/MCM-41 catalyst. Based on the analysis using the degree of rate control (DRC) method, the authors proposed that on RhCo₃/MCM-41, the first step of olefin hydrogenation to alkyl was kinetically irrelevant to ethylene hydroformylation, but was influential to the activity of propylene hydroformylation. This result demonstrated that both catalysts and reactants would influence the surface reaction mechanism and even changed the RDS, which required a case-by case study of the heterogeneous hydroformylation mechanism. For long-chain linear α -olefins, some catalysts have been evaluated under the same conditions (**Figure 11e**), and the length of carbon chain showed basically no influence on the hydroformylation activity, indicating that long-chain α -olefins shared some commonalities in reaction mechanisms, especially in the aspect of catalytic activity. However, some catalysts with encapsulation structure showed differences because the pores could selectively permit some

reactants to diffuse while prohibit the others. This difference originated from the various transfer properties of catalyst structure instead of the different reaction mechanisms.

Secondly, we would like to discuss the chemoselectivity. **Figure 11a** summarized the average chemoselectivity for hydroformylation reactions of different reactants. Many data points of ethylene and propylene hydroformylation located below 80%, indicating that chemoselectivity was a major concern for hydroformylation of light olefins. However, with increasing carbon chain, the average chemoselectivity increased to >90%, demonstrating that the side reaction of hydrogenation was no longer a major challenge for hydroformylation of 1-butene, 1-hexene, 1-octene and styrene. As discussed above, we speculated that the modification by organic phosphines and the existence of solvent could significantly enhance the chemoselectivity against hydrogenation. The nature of the reactants with longer carbon chain made it easier to obtain a high chemoselectivity primarily originated from the competitive reaction of CO and H₂. Thus, the modification of CO adsorption energy and activation energy of CO insertion would influence the chemoselectivity, which was mainly realized by regulating the electronic structure of Rh active sites.

Thirdly, in terms of the regioselectivity, all reactants showed a trade-off between activity and regioselectivity (**Figure 11b**). Regardless of the selectivity improvement to either linear or branched aldehydes, the catalytic activity was sacrificed to a certain extent. The highest TOF was always obtained near the $l/b=1$ line for both linear α -olefins and styrene hydroformylation reactions. Also, the terminal α -olefins showed a tendency to produce linear aldehydes, with most of the data points located above the $l/b=1$ line. On the contrary, styrene tended to produce more branched products with most of the points located below the $l/b=1$ line. The average value of l/b ratio confirmed the trend (**Figure 11c**). By comparing hydroformylation reactions on the same

catalysts, this trend was even more obvious (**Figure 11d**). All catalysts showed a significantly decline in the value of l/b ratio, when changing the reactants from α -olefins to styrene. As for the α -olefins with different carbon chain length, their regioselectivity basically kept constant on a given catalyst. One exception was the Rh₂O₃@S-1 catalyst,⁴⁹ where a volcanic relationship was observed between the l/b ratio and carbon chain length. This was attributed to the long-range steric hindrance of the S-1 shell, which suppressed the diffusion of long chain reactants. The l/b ratio slightly decreased for 1-dodecene, together with a significant decline of aldehyde yields (**Figure 11e**). This was because 1-dodecene was too long to access the encapsulated Rh sites, and was directly converted on the leached compounds. The other exception was the RhCoHT-1 catalyst,⁵⁰ but the authors did not explain the strange U-shaped curve, which required further investigation. Moreover, we would like to discuss the modification strategy of regioselectivity. As motioned above, both electronic effects and steric hindrance would influence the product distribution. The electronic structure could be tuned by synthesizing SACs,³⁵ doping with secondary metals,⁷⁷ and adding functional groups to phosphine ligands.³¹ The steric hindrance could be divided into long-range and short-range hindrance. The former changed the diffusion properties of reactants and/or products, and was usually realized by encapsulation,^{46–49} while the latter tuned the local environment around Rh by adding inorganic metals,³⁰ modifying surface functional groups⁴³ or changing suitable phosphine ligands.^{4,33,55,56,76,79} The adsorption geometry of reactants was then limited by the steric hindrance and the regioselectivity could be enhanced. Apart from the modification of catalysts, the reaction conditions, including temperature,^{31,49,55,57,74,92} syngas pressure^{41,50} and solvents,^{41,85,86} also needed to be optimized for a specific catalyst to maximize the regioselectivity.

Fourthly, the enantioselectivity could only be enhanced by adding chiral ligands. In this regard, homogeneous catalysts possessed great advantages due to the diversity of phosphine ligands, which could provide different electronic and steric hindrance environment. At present, research on heterogeneous systems is still very limited, which is possibly a potential opportunity for future studies.

Finally, the catalyst stability is an essential challenge, due to the strong coordination between Rh metals and CO. In gaseous reactions, such as the hydroformylation of ethylene and propylene, the challenge of stability is not serious, because the carbonyl complex of Rh is not stable at relatively high temperatures. For long chain olefins and aromatic olefins, however, the leaching of Rh to the liquid phase is severe. One of the solutions is to enhance the interaction between Rh atoms and the support. The Rh-Xantphos/POPs-PPh₃ catalysts were reported to be stable for 1-octene hydroformylation in a continuous fixed-bed test for over 400 h, due to the strong coordination between Rh sites and phosphine ligands.⁵⁵ Similarly, the Rh/phosphite-POP catalysts were also stable in 2-octene hydroformylation for over 12 runs.¹⁰⁷ Yan et al.⁹³ used ionic liquid to bridge the Rh sites and TiO₂ supports, which immobilized the Rh metals and enhanced the stability. Moreover, the encapsulation can improve the stability. The recyclability of silicalite-1 encapsulated Rh catalysts was significantly enhanced in comparison to the supported counterparts.⁴⁹ The reaction conditions would also influence the catalysts recyclability by changing the stability of carbonyl complex. So far, the stability of heterogeneous hydroformylation catalysts has not been systematically studied, and requires more investigations.

The hydroformylation reactions of other functionalized alkenes, such as norbornene,¹⁰⁸ vinyl acetate^{36,109} and diisobutene,⁷⁰ have also attracted much attention. The main challenges faced by these reactants can still be categorized into activity, selectivity and stability, as mentioned above.

The provided modification toolbox, including electronic modification, steric hindrance and condition optimization, should still be applicable to the hydroformylation reactions of these alkenes.

8. Conclusions and future perspectives

Hydroformylation using heterogeneous catalysts avoids the difficulty of separation, which reduces the discharge of phosphine-containing wastes and the loss of precious metals in homogeneous systems, making heterogeneous hydroformylation reactions more environmentally friendly. In this review, we have summarized the recent development of Rh-based heterogeneous hydroformylation in the last decade and the modification strategies can be classified into three aspects: electronic effects, steric hindrance and reaction condition optimization.

Different olefin reactants face different major challenges and require corresponding modification strategies. For ethylene hydroformylation, the major concern is the chemoselectivity against hydrogenation, and the main solutions are to tune the electronic structure of catalysts and to introduce some solvents. For styrene and linear α -olefins ($>C_4$) hydroformylation, the major challenge is the regioselectivity, which is affected by local environment (electronic and steric) and reaction conditions (temperature and pressure). The steric hindrance can be further divided as long-range and short-range hindrance, which influences the diffusion and adsorption properties directly, and therefore changes the l/b ratio. For propylene hydroformylation, both chemoselectivity and regioselectivity are important, requiring the researchers to seek a balance between them.

Moreover, we have summarized the catalytic performance of different catalysts and plotted the envelope curve for the various reactants, which allows researchers to locate their new catalysts

more easily, and further breakthroughs should be aimed to push the envelope outward. The catalysts should have either higher selectivity when the activity is the same, or higher activity when the selectivity is comparable. Furthermore, the reaction mechanism and solvent effects in heterogeneous hydroformylation require further study. The stability of heterogeneous catalysts is also an important challenge for future industrial application and requires more investigations.

Finally, a fundamental understanding of the structure-performance relationship is critical for the design of next-generation heterogeneous hydroformylation catalysts. The understanding of such relationship requires combined the efforts of (1) careful kinetic measurements of reaction orders and apparent activation energies performed without transport limitations, (2) *in situ* characterization of the electronic and structural properties of catalysts under hydroformylation reaction conditions using synchrotron-based XRD, XANES and EXAFS, (3) identification of surface reaction intermediates using *in situ* vibrational spectroscopies, and (4) in-depth DFT calculations of hydroformylation reaction networks using relevant structural models identified from the *in situ* experimental measurements. Such combined studies have not been performed on most of the heterogeneous hydroformylation systems and represent important future research opportunities.

ACKNOWLEDGMENT

Authors from Tsinghua University acknowledge financial support from the National Natural Science Foundation of China (Grant No. 22178195). Authors from Columbia University acknowledge support from the United States Department of Energy, Office of Basic Energy Sciences, Catalysis Science Program (Grant No. DE-SC0012704).

AUTHOR INFORMATION

Corresponding Authors

*Corresponding authors: Jingguang Chen, jgchen@columbia.edu; Tiefeng Wang, wangtf@tsinghua.edu.cn.

Author contributions

Writing—original draft, B.L.; writing—review and editing, Y.W., N.H., X.L., Z.X., J.C. and T.W.; supervision, J.C. and T.W.; funding acquisition, J.C. and T.W.

DECLARATION OF INTERESTS

The authors declare no competing financial interest.

REFERENCES

1. Franke, R., Selent, D., and Börner, A. (2012). Applied Hydroformylation. *Chem. Rev.* *112*, 5675–5732.
2. Peng, J.-B., Geng, H.-Q., and Wu, X.-F. (2019). The Chemistry of CO: Carbonylation. *Chem* *5*, 526–552.
3. Armanino, N., Charpentier, J., Flachsmann, F., Goetze, A., Liniger, M., and Kraft, P. (2020). What's Hot, What's Not: The Trends of the Past 20 Years in the Chemistry of Odorants. *Angew. Chem. Int. Ed.* *59*, 16310–16344.
4. Gao, P., Liang, G., Ru, T., Liu, X., Qi, H., Wang, A., and Chen, F.-E. (2021). Phosphorus coordinated Rh single-atom sites on nanodiamond as highly regioselective catalyst for hydroformylation of olefins. *Nat. Commun.* *12*, 4698.
5. Hood, D.M., Johnson, R.A., Carpenter, A.E., Younker, J.M., Vinyard, D.J., and Stanley, G.G. (2020). Highly active cationic cobalt(II) hydroformylation catalysts. *Science* *367*, 542–548.
6. Brezny, A.C., and Landis, C.R. (2018). Recent Developments in the Scope, Practicality, and Mechanistic Understanding of Enantioselective Hydroformylation. *Acc. Chem. Res.* *51*, 2344–2354.
7. Chakraborty, S., Almasalma, A.A., and de Vries, J.G. (2021). Recent developments in asymmetric hydroformylation. *Catal. Sci. Technol.* *11*, 5388–5411.
8. Bauder, C., and Sémeril, D. (2019). Styrene Hydroformylation with Cavity-Shaped Ligands: Styrene Hydroformylation with Cavity-Shaped Ligands. *Eur. J. Inorg. Chem.* *2019*, 4951–4965.
9. Tewari, T., Kumar, R., Chandanshive, A.C., and Chikkali, S.H. (2021). Phosphorus Ligands in Hydroformylation and Hydrogenation: A Personal Account. *Chem. Rec.* *21*, 1182–1198.
10. Cole-Hamilton, D.J. (2003). Homogeneous Catalysis--New Approaches to Catalyst Separation, Recovery, and Recycling. *Science* *299*, 1702–1706.
11. Kumar, R., and Chikkali, S.H. (2022). Hydroformylation of olefins by metals other than rhodium. *J. Organomet. Chem.* *960*, 122231.
12. Navidi, N., Marin, G.B., and Thybaut, J.W. (2016). A Single-Event Microkinetic model for ethylene hydroformylation to propanal on Rh and Co based catalysts. *Appl. Catal. Gen.* *524*, 32–44.
13. Xie, Z., Xu, Y., Xie, M., Chen, X., Lee, J.H., Stavitski, E., Kattel, S., and Chen, J.G. (2020). Reactions of CO₂ and ethane enable CO bond insertion for production of C₃ oxygenates. *Nat. Commun.* *11*, 1887.
14. Liu, S., Dai, X., Wang, H., Wang, X., and Shi, F. (2020). Organic Ligand-Free Hydroformylation with Rh Particles as Catalyst. *Chin. J. Chem.* *38*, 139–143.

15. Yamagishi, T., Ito, S., Tomishige, K., and Kunimori, K. (2005). Selective formation of 1-propanol via ethylene hydroformylation over the catalyst originated from RhVO₄. *Catal. Commun.* *6*, 421–425.
16. Navidi, N., Thybaut, J.W., and Marin, G.B. (2014). Experimental investigation of ethylene hydroformylation to propanal on Rh and Co based catalysts. *Appl. Catal. Gen.* *469*, 357–366.
17. Huang, N., Liu, B., Lan, X., and Wang, T. (2020). Insights into the Bimetallic Effects of a RhCo Catalyst for Ethene Hydroformylation: Experimental and DFT Investigations. *Ind. Eng. Chem. Res.* *59*, 18771–18780.
18. Ro, I., Xu, M., Graham, G.W., Pan, X., and Christopher, P. (2019). Synthesis of Heteroatom Rh–ReO_x Atomically Dispersed Species on Al₂O₃ and Their Tunable Catalytic Reactivity in Ethylene Hydroformylation. *ACS Catal.* *9*, 10899–10912.
19. Liu, J., Yan, L., Ding, Y., Jiang, M., Dong, W., Song, X., Liu, T., and Zhu, H. (2015). Promoting effect of Al on tethered ligand-modified Rh/SiO₂ catalysts for ethylene hydroformylation. *Appl. Catal. Gen.* *492*, 127–132.
20. Huang, N., Liu, B., Lan, X., Yan, B., and Wang, T. (2021). Promotion of diphosphine ligands (PPh₂(CH₂)_nPPh₂, n = 1, 2, 3, 5, 6) for supported Rh/SiO₂ catalysts in heterogeneous ethene hydroformylation. *Mol. Catal.* *511*, 111736.
21. Weiß, A., Giese, M., Lijewski, M., Franke, R., Wasserscheid, P., and Haumann, M. (2017). Modification of nitrogen doped carbon for SILP catalyzed hydroformylation of ethylene. *Catal. Sci. Technol.* *7*, 5562–5571.
22. Jiang, M., Yan, L., Ding, Y., Sun, Q., Liu, J., Zhu, H., Lin, R., Xiao, F., Jiang, Z., and Liu, J. (2015). Ultrastable 3V-PPh₃ polymers supported single Rh sites for fixed-bed hydroformylation of olefins. *J. Mol. Catal. Chem.* *404–405*, 211–217.
23. Alvarado Rupflin, L., Mormul, J., Lejkowski, M., Titlbach, S., Papp, R., Gläser, R., Dimitrakopoulou, M., Huang, X., Trunschke, A., Willinger, M.G., et al. (2017). Platinum Group Metal Phosphides as Heterogeneous Catalysts for the Gas-Phase Hydroformylation of Small Olefins. *ACS Catal.* *7*, 3584–3590.
24. Lee, S., Patra, A., Christopher, P., Vlachos, D.G., and Caratzoulas, S. (2021). Theoretical Study of Ethylene Hydroformylation on Atomically Dispersed Rh/Al₂O₃ Catalysts: Reaction Mechanism and Influence of the ReO_x Promoter. *ACS Catal.* *11*, 9506–9518.
25. Ding, Y., Yan, L., and Song, X. (2022). The Multifunctional Materials for Heterogenous Carboxylation: From Fundamental Understanding to Industrial Applications. In *The Chemical Transformations of C1 Compounds* (John Wiley & Sons), p. 292.
26. Hanf, S., Alvarado Rupflin, L., Gläser, R., and Schunk, S. (2020). Current State of the Art of the Solid Rh-Based Catalyzed Hydroformylation of Short-Chain Olefins. *Catalysts* *10*, 510.

27. Sordelli, L. (2003). Characterization and catalytic performances of alkali-metal promoted Rh/SiO₂ catalysts for propene hydroformylation. *J. Mol. Catal. Chem.* *204–205*, 509–518.
28. Tomishige, K., Furikado, I., Yamagishi, T., Ito, S., and Kunimori, K. (2005). Promoting Effect of Mo on Alcohol Formation in Hydroformylation of Propylene and Ethylene on Mo-Rh/SiO₂. *Catal. Lett.* *103*, 15–21.
29. Yamagishi, T., Furikado, I., Ito, S., Miyao, T., Naito, S., Tomishige, K., and Kunimori, K. (2006). Catalytic performance and characterization of RhVO₄/SiO₂ for hydroformylation and CO hydrogenation. *J. Mol. Catal. Chem.* *244*, 201–212.
30. Zhang, J., Sun, P., Gao, G., Wang, J., Zhao, Z., Muhammad, Y., and Li, F. (2020). Enhancing regioselectivity via tuning the microenvironment in heterogeneous hydroformylation of olefins. *J. Catal.* *387*, 196–206.
31. Shylesh, S., Hanna, D., Mlinar, A., Kōng, X.-Q., Reimer, J.A., and Bell, A.T. (2013). In Situ Formation of Wilkinson-Type Hydroformylation Catalysts: Insights into the Structure, Stability, and Kinetics of Triphenylphosphine- and Xantphos-Modified Rh/SiO₂. *ACS Catal.* *3*, 348–357.
32. Weiß, A., Munoz, M., Haas, A., Rietzler, F., Steinrück, H.-P., Haumann, M., Wasserscheid, P., and Etzold, B.J.M. (2016). Boosting the Activity in Supported Ionic Liquid-Phase-Catalyzed Hydroformylation via Surface Functionalization of the Carbon Support. *ACS Catal.* *6*, 2280–2286.
33. Li, C., Yan, L., Lu, L., Xiong, K., Wang, W., Jiang, M., Liu, J., Song, X., Zhan, Z., Jiang, Z., et al. (2016). Single atom dispersed Rh-biphephos@PPH₃@porous organic copolymers: highly efficient catalysts for continuous fixed-bed hydroformylation of propene. *Green Chem.* *18*, 2995–3005.
34. Zhao, K., Wang, H., Wang, X., Li, T., Dai, X., Zhang, L., Cui, X., and Shi, F. (2021). Confinement of atomically dispersed Rh catalysts within porous monophosphine polymers for regioselective hydroformylation of alkenes. *J. Catal.* *401*, 321–330.
35. Wang, L., Zhang, W., Wang, S., Gao, Z., Luo, Z., Wang, X., Zeng, R., Li, A., Li, H., Wang, M., et al. (2016). Atomic-level insights in optimizing reaction paths for hydroformylation reaction over Rh/CoO single-atom catalyst. *Nat. Commun.* *7*, 14036.
36. Chuai, H., Su, P., Liu, H., Zhu, B., Zhang, S., and Huang, W. (2019). Alkali and Alkaline Earth Cation-Decorated TiO₂ Nanotube-Supported Rh Catalysts for Vinyl Acetate Hydroformylation. *Catalysts* *9*, 194.
37. Kaiser, S.K., Chen, Z., Faust Akl, D., Mitchell, S., and Pérez-Ramírez, J. (2020). Single-Atom Catalysts across the Periodic Table. *Chem. Rev.* *120*, 11703–11809.
38. Li, Z., Ji, S., Liu, Y., Cao, X., Tian, S., Chen, Y., Niu, Z., and Li, Y. (2020). Well-Defined Materials for Heterogeneous Catalysis: From Nanoparticles to Isolated Single-Atom Sites. *Chem. Rev.* *120*, 623–682.

39. Li, X., Qin, T., Li, L., Wu, B., Lin, T., and Zhong, L. (2021). One-pot Synthesis of Acetals by Tandem Hydroformylation-acetalization of Olefins Using Heterogeneous Supported Catalysts. *Catal. Lett.* *151*, 2638–2646.
40. Kontkanen, M.-L., Tuikka, M., Kinnunen, N., Suvanto, S., and Haukka, M. (2013). Hydroformylation of 1-Hexene over Rh/Nano-Oxide Catalysts. *Catalysts* *3*, 324–337.
41. Jagtap, S.A., Bhosale, M.A., Sasaki, T., and Bhanage, B.M. (2016). Rh/Cu₂O nanoparticles: Synthesis, characterization and catalytic application as a heterogeneous catalyst in hydroformylation reaction. *Polyhedron* *120*, 162–168.
42. Tan, M., Yang, G., Wang, T., Vitidsant, T., Li, J., Wei, Q., Ai, P., Wu, M., Zheng, J., and Tsubaki, N. (2016). Active and regioselective rhodium catalyst supported on reduced graphene oxide for 1-hexene hydroformylation. *Catal. Sci. Technol.* *6*, 1162–1172.
43. Tan, M., Wang, D., Ai, P., Liu, G., Wu, M., Zheng, J., Yang, G., Yoneyama, Y., and Tsubaki, N. (2016). Enhancing catalytic performance of activated carbon supported Rh catalyst on heterogeneous hydroformylation of 1-hexene via introducing surface oxygen-containing groups. *Appl. Catal. Gen.* *527*, 53–59.
44. Li, X., Zhang, Y., Meng, M., Yang, G., San, X., Takahashi, M., and Tsubaki, N. (2010). Silicalite-1 membrane encapsulated Rh/activated-carbon catalyst for hydroformylation of 1-hexene with high selectivity to normal aldehyde. *J. Membr. Sci.* *347*, 220–227.
45. Hou, C., Zhao, G., Ji, Y., Niu, Z., Wang, D., and Li, Y. (2014). Hydroformylation of alkenes over rhodium supported on the metal-organic framework ZIF-8. *Nano Res.* *7*, 1364–1369.
46. Vu, T.V., Kosslick, H., Schulz, A., Harloff, J., Paetzold, E., Lund, H., Kragl, U., Schneider, M., and Fulda, G. (2012). Influence of the textural properties of Rh/MOF-5 on the catalytic properties in the hydroformylation of olefins. *Microporous Mesoporous Mater.* *154*, 100–106.
47. Van Vu, T., Kosslick, H., Schulz, A., Harloff, J., Paetzold, E., Schneider, M., Radnik, J., Steinfeldt, N., Fulda, G., and Kragl, U. (2013). Selective hydroformylation of olefins over the rhodium supported large porous metal–organic framework MIL-101. *Appl. Catal. Gen.* *468*, 410–417.
48. Van Vu, T., Kosslick, H., Schulz, A., Harloff, J., Paetzold, E., Radnik, J., Kragl, U., Fulda, G., Janiak, C., and Tuyen, N.D. (2013). Hydroformylation of olefins over rhodium supported metal-organic framework catalysts of different structure. *Microporous Mesoporous Mater.* *177*, 135–142.
49. Liu, C., Zhang, J., Liu, H., Qiu, J., and Zhang, X. (2019). Heterogeneous Ligand-Free Rhodium Oxide Catalyst Embedded within Zeolitic Microchannel to Enhance Regioselectivity in Hydroformylation. *Ind. Eng. Chem. Res.* *58*, 21285–21295.

50. Sharma, D., Ganesh, V., and Sakthivel, A. (2018). Rhodium incorporated monometallic cobalt hydrotalcite-type materials: Preparation and its applications for the hydroformylation of alkenes. *Appl. Catal. Gen.* *555*, 155–160.
51. Zhu, H.J., Ding, Y.J., Yan, L., Xiong, J.M., Lu, Y., and Lin, L.W. (2004). The PPh₃ ligand modified Rh/SiO₂ catalyst for hydroformylation of olefins. *Catal. Today* *93–95*, 389–393.
52. Tan, M., Ishikuro, Y., Hosoi, Y., Yamane, N., Ai, P., Zhang, P., Yang, G., Wu, M., Yang, R., and Tsubaki, N. (2017). PPh₃ functionalized Rh/rGO catalyst for heterogeneous hydroformylation: Bifunctional reduction of graphene oxide by organic ligand. *Chem. Eng. J.* *330*, 863–869.
53. Ganga, V.S.R., Dabbawala, A.A., Munusamy, K., Abdi, S.H.R., Kureshy, R.I., Khan, N.H., and Bajaj, H.C. (2016). Rhodium complexes supported on nanoporous activated carbon for selective hydroformylation of olefins. *Catal. Commun.* *84*, 21–24.
54. Sharma, S.K., Parikh, P.A., and Jasra, R.V. (2010). Hydroformylation of alkenes using heterogeneous catalyst prepared by intercalation of HRh(CO)(TPPTS)₃ complex in hydrotalcite. *J. Mol. Catal. Chem.* *316*, 153–162.
55. Li, C., Sun, K., Wang, W., Yan, L., Sun, X., Wang, Y., Xiong, K., Zhan, Z., Jiang, Z., and Ding, Y. (2017). Xantphos doped Rh/POPs-PPh₃ catalyst for highly selective long-chain olefins hydroformylation: Chemical and DFT insights into Rh location and the roles of Xantphos and PPh₃. *J. Catal.* *353*, 123–132.
56. Jia, X., Liang, Z., Chen, J., Lv, J., Zhang, K., Gao, M., Zong, L., and Xie, C. (2019). Porous Organic Polymer Supported Rhodium as a Reusable Heterogeneous Catalyst for Hydroformylation of Olefins. *Org. Lett.* *21*, 2147–2150.
57. Wang, Z., and Yang, Y. (2020). Rh-catalyzed highly regioselective hydroformylation to linear aldehydes by employing porous organic polymer as a ligand. *RSC Adv.* *10*, 29263–29267.
58. Galdeano-Ruano, C., Lopes, C.W., Motta Meira, D., Corma, A., and Oña-Burgos, P. (2021). Rh₂P Nanoparticles Stabilized by Carbon Patches for Hydroformylation of Olefins. *ACS Appl. Nano Mater.* *4*, 10743–10753.
59. Gorbunov, D., Safronova, D., Kardasheva, Y., Maximov, A., Rosenberg, E., and Karakhanov, E. (2018). New Heterogeneous Rh-Containing Catalysts Immobilized on a Hybrid Organic–Inorganic Surface for Hydroformylation of Unsaturated Compounds. *ACS Appl. Mater. Interfaces* *10*, 26566–26575.
60. Dong, K., Sun, Q., Tang, Y., Shan, C., Aguila, B., Wang, S., Meng, X., Ma, S., and Xiao, F.-S. (2019). Bio-inspired creation of heterogeneous reaction vessels via polymerization of supramolecular ion pair. *Nat. Commun.* *10*, 3059.
61. Lang, R., Du, X., Huang, Y., Jiang, X., Zhang, Q., Guo, Y., Liu, K., Qiao, B., Wang, A., and Zhang, T. (2020). Single-Atom Catalysts Based on the Metal–Oxide Interaction. *Chem. Rev.* *120*, 11986–12043.

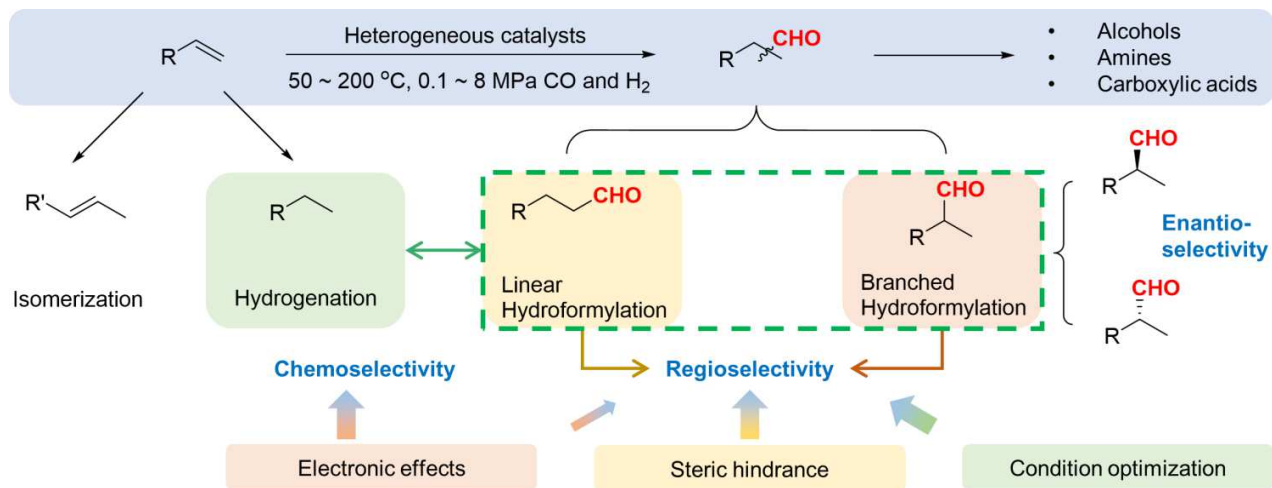
62. Li, C., Xiong, K., Yan, L., Jiang, M., Song, X., Wang, T., Chen, X., Zhan, Z., and Ding, Y. (2016). Designing highly efficient Rh/CPOL-bp&PPh₃ heterogenous catalysts for hydroformylation of internal and terminal olefins. *Catal. Sci. Technol.* *6*, 2143–2149.
63. Bauer, G., Ongari, D., Tiana, D., Gäumann, P., Rohrbach, T., Pareras, G., Tarik, M., Smit, B., and Ranocchiari, M. (2020). Metal-organic frameworks as kinetic modulators for branched selectivity in hydroformylation. *Nat. Commun.* *11*, 1059.
64. Pilaski, M., Artz, J., Islam, H.-U., Beale, A.M., and Palkovits, R. (2016). N-containing covalent organic frameworks as supports for rhodium as transition-metal catalysts in hydroformylation reactions. *Microporous Mesoporous Mater.* *227*, 219–227.
65. Vunain, E., Ncube, P., Jalama, K., and Meijboom, R. (2018). Confinement effect of rhodium(I) complex species on mesoporous MCM-41 and SBA-15: effect of pore size on the hydroformylation of 1-octene. *J. Porous Mater.* *25*, 303–320.
66. Ji, G., Li, C., Xiao, D., Wang, G., Sun, Z., Jiang, M., Hou, G., Yan, L., and Ding, Y. (2021). The effect of the position of cross-linkers on the structure and microenvironment of PPh₃ moiety in porous organic polymers. *J. Mater. Chem. A* *9*, 9165–9174.
67. Gorbunov, D., Nenasheva, M., Naranov, E., Maximov, A., Rosenberg, E., and Karakhanov, E. (2021). Tandem hydroformylation/hydrogenation over novel immobilized Rh-containing catalysts based on tertiary amine-functionalized hybrid inorganic-organic materials. *Appl. Catal. Gen.* *623*, 118266.
68. Sun, Q., Jiang, M., Shen, Z., Jin, Y., Pan, S., Wang, L., Meng, X., Chen, W., Ding, Y., Li, J., et al. (2014). Porous organic ligands (POLs) for synthesizing highly efficient heterogeneous catalysts. *Chem. Commun.* *50*, 11844–11847.
69. Sartipi, S., Valero Romero, M.J., Rozhko, E., Que, Z., Stil, H.A., de With, J., Kapteijn, F., and Gascon, J. (2015). Dynamic Release-Immobilization of a Homogeneous Rhodium Hydroformylation Catalyst by a Polyoxometalate Metal-Organic Framework Composite. *ChemCatChem* *7*, 3243–3247.
70. Wang, H., Yuan, H., Chen, X., Wang, X., Zhao, K., and Shi, F. (2022). A Highly Active N-Doped Carbon Supported CoFe Alloy Catalyst for Hydroformylation of C₈ Olefins. *J. Phys. Chem. C* *126*, 273–281.
71. Garcia, M.A.S., Oliveira, K.C.B., Costa, J.C.S., Corio, P., and Gusevskaya, E.V. (2015). Rhodium Nanoparticles as Precursors for the Preparation of an Efficient and Recyclable Hydroformylation Catalyst. *ChemCatChem* *7*, 1566–1572.
72. Rodrigues, F.M.S., Dias, L.D., Calvete, M.J.F., Maria, T.M.R., Rossi, L.M., Pombeiro, A.J.L., Martins, L.M.D.R.S., and Pereira, M.M. (2021). Immobilization of Rh(I)-N-Xantphos and Fe(II)-C-Scorpionate onto Magnetic Nanoparticles: Reusable Catalytic System for Sequential Hydroformylation/Acetalization. *Catalysts* *11*, 608.

73. Omosun, N.N., Ngubane, S., and Smith, G.S. (2021). Hydroformylation of olefins using redox-active rhodium(I) alpha-diimine-cored aryl ether metallodendrimers. *Appl. Catal. Gen.* *610*, 117950.
74. Sun, Q., Dai, Z., Liu, X., Sheng, N., Deng, F., Meng, X., and Xiao, F.-S. (2015). Highly Efficient Heterogeneous Hydroformylation over Rh-Metalated Porous Organic Polymers: Synergistic Effect of High Ligand Concentration and Flexible Framework. *J. Am. Chem. Soc.* *137*, 5204–5209.
75. Verheyen, T., Santillo, N., Marinelli, D., Petricci, E., De Borggraeve, W.M., Vaccaro, L., and Smet, M. (2019). An Effective and Reusable Hyperbranched Polymer Immobilized Rhodium Catalyst for the Hydroformylation of Olefins. *ACS Appl. Polym. Mater.* *1*, 1496–1504.
76. Wang, W., Li, C., Zhang, H., Zhang, J., Lu, L., Jiang, Z., Cui, L., Liu, H., Yan, L., and Ding, Y. (2021). Enhancing the activity, selectivity, and recyclability of Rh/PPh₃ system-catalyzed hydroformylation reactions through the development of a PPh₃-derived quasi-porous organic cage as a ligand. *Chin. J. Catal.* *42*, 1216–1226.
77. Wei, B., Liu, X., Hua, K., Deng, Y., Wang, H., and Sun, Y. (2021). Effectively Regulating the Microenvironment of Atomically Dispersed Rh through Co and Pi to Promote the Selectivity in Olefin Hydroformylation. *ACS Appl. Mater. Interfaces* *13*, 15113–15121.
78. Chen, L., Tian, J., Song, H., Gao, Z., Wei, H., Wang, W., and Ren, W. (2020). Enhancing the stability of the Rh/ZnO catalyst by the growth of ZIF-8 for the hydroformylation of higher olefins. *RSC Adv.* *10*, 34381–34386.
79. Han, D., Li, X., Zhang, H., Liu, Z., Hu, G., and Li, C. (2008). Asymmetric hydroformylation of olefins catalyzed by rhodium nanoparticles chirally stabilized with (R)-BINAP ligand. *J. Mol. Catal. Chem.* *283*, 15–22.
80. Alini, S., Bottino, A., Capannelli, G., Comite, A., and Paganelli, S. (2005). Preparation and characterisation of Rh/Al₂O₃ catalysts and their application in the adiponitrile partial hydrogenation and styrene hydroformylation. *Appl. Catal. Gen.* *292*, 105–112.
81. Shi, Y., Hu, X., Chen, L., Lu, Y., Zhu, B., Zhang, S., and Huang, W. (2017). Boron modified TiO₂ nanotubes supported Rh-nanoparticle catalysts for highly efficient hydroformylation of styrene. *New J. Chem.* *41*, 6120–6126.
82. Shi, Y., Ji, G., Hu, Q., Lu, Y., Hu, X., Zhu, B., and Huang, W. (2020). Highly uniform Rh nanoparticles supported on boron doped g-C₃N₄ as a highly efficient and recyclable catalyst for heterogeneous hydroformylation of alkenes. *New J. Chem.* *44*, 20–23.
83. Shi, Y., Lu, Y., Ren, T., Li, J., Hu, Q., Hu, X., Zhu, B., and Huang, W. (2020). Rh Particles Supported on Sulfated g-C₃N₄: A Highly Efficient and Recyclable Heterogeneous Catalyst for Alkene Hydroformylation. *Catalysts* *10*, 1359.
84. Han, D., Li, X., Zhang, H., Liu, Z., Li, J., and Li, C. (2006). Heterogeneous asymmetric hydroformylation of olefins on chirally modified Rh/SiO₂ catalysts. *J. Catal.* *243*, 318–328.

85. Abu-Reziq, R., Alper, H., Wang, D., and Post, M.L. (2006). Metal Supported on Dendronized Magnetic Nanoparticles: Highly Selective Hydroformylation Catalysts. *J. Am. Chem. Soc.* *128*, 5279–5282.
86. Shaikh, M.N., Aziz, Md.A., Helal, A., Bououdina, M., Yamani, Z.H., and Kim, T.-J. (2016). Magnetic nanoparticle-supported ferrocenylphosphine: a reusable catalyst for hydroformylation of alkene and Mizoroki–Heck olefination. *RSC Adv.* *6*, 41687–41695.
87. Liu, Y., Dikhtiarenko, A., Xu, N., Sun, J., Tang, J., Wang, K., Xu, B., Tong, Q., Heeres, H.J., He, S., et al. (2020). Triphenylphosphine-Based Covalent Organic Frameworks and Heterogeneous Rh-P-COFs Catalysts. *Chem. – Eur. J.* *26*, 12134–12139.
88. Sun, Q., Dai, Z., Meng, X., and Xiao, F.-S. (2017). Enhancement of hydroformylation performance via increasing the phosphine ligand concentration in porous organic polymer catalysts. *Catal. Today* *298*, 40–45.
89. Wang, T., Wang, W., Lyu, Y., Xiong, K., Li, C., Zhang, H., Zhan, Z., Jiang, Z., and Ding, Y. (2017). Porous Rh/BINAP polymers as efficient heterogeneous catalysts for asymmetric hydroformylation of styrene: Enhanced enantioselectivity realized by flexible chiral nanopockets. *Chin. J. Catal.* *38*, 691–698.
90. Lang, R., Li, T., Matsumura, D., Miao, S., Ren, Y., Cui, Y.-T., Tan, Y., Qiao, B., Li, L., Wang, A., et al. (2016). Hydroformylation of Olefins by a Rhodium Single-Atom Catalyst with Activity Comparable to $\text{RhCl}(\text{PPh}_3)_3$. *Angew. Chem. Int. Ed.* *55*, 16054–16058.
91. Li, T., Chen, F., Lang, R., Wang, H., Su, Y., Qiao, B., Wang, A., and Zhang, T. (2020). Styrene Hydroformylation with In Situ Hydrogen: Regioselectivity Control by Coupling with the Low-Temperature Water–Gas Shift Reaction. *Angew. Chem. Int. Ed.* *59*, 7430–7434.
92. Amsler, J., Sarma, B.B., Agostini, G., Prieto, G., Plessow, P.N., and Studt, F. (2020). Prospects of Heterogeneous Hydroformylation with Supported Single Atom Catalysts. *J. Am. Chem. Soc.* *142*, 5087–5096.
93. Ding, S., Hülsey, M.J., An, H., He, Q., Asakura, H., Gao, M., Hasegawa, J., Tanaka, T., and Yan, N. (2021). Ionic Liquid-Stabilized Single-Atom Rh Catalyst Against Leaching. *CCS Chem.*, 1814–1822.
94. Tang, P., Paganelli, S., Carraro, F., Blanco, M., Riccò, R., Marega, C., Badocco, D., Pastore, P., Doonan, C.J., and Agnoli, S. (2020). Postsynthetic Metalated MOFs as Atomically Dispersed Catalysts for Hydroformylation Reactions. *ACS Appl. Mater. Interfaces* *12*, 54798–54805.
95. Liu, B., Huang, N., Wang, Y., Lan, X., and Wang, T. (2021). Promotion of Inorganic Phosphorus on Rh Catalysts in Styrene Hydroformylation: Geometric and Electronic Effects. *ACS Catal.* *11*, 1787–1796.
96. Liu, B., Wang, Y., Huang, N., Lan, X., and Wang, T. (2021). Activity Promotion of $\text{Rh}_8\text{-}_x\text{Co}_x\text{P}_4$ Bimetallic Phosphides in Styrene Hydroformylation: Dual Influence of Adsorption and Surface Reaction. *ACS Catal.* *11*, 9850–9859.

97. Liu, B., Huang, N., Wang, Y., Lan, X., and Wang, T. (2022). Regioselectivity regulation of styrene hydroformylation over Rh-based Phosphides: Combination of DFT calculations and kinetic studies. *Chem. Eng. J.* *441*, 136101.
98. Pignolet, L.M. (2013). *Homogeneous catalysis with metal phosphine complexes* (Springer Science & Business Media).
99. Delolo, F.G., dos Santos, E.N., and Gusevskaya, E.V. (2019). Anisole: a further step to sustainable hydroformylation. *Green Chem.* *21*, 1091–1098.
100. Jameel, F., and Stein, M. (2021). Solvent effects in hydroformylation of long-chain olefins. *Mol. Catal.* *503*, 111429.
101. Mao, Z., Xie, Z., and Chen, J.G. (2021). Comparison of Heterogeneous Hydroformylation of Ethylene and Propylene over RhCo₃/MCM-41 Catalysts. *ACS Catal.*, 14575–14585.
102. Wang, Y., Yan, L., Li, C., Jiang, M., Zhao, Z., Hou, G., and Ding, Y. (2018). Heterogeneous Rh/CPOL-BP&P(OPh)₃ catalysts for hydroformylation of 1-butene: The formation and evolution of the active species. *J. Catal.* *368*, 197–206.
103. Wang, Y., Yan, L., Li, C., Jiang, M., Wang, W., and Ding, Y. (2018). Highly efficient porous organic copolymer supported Rh catalysts for heterogeneous hydroformylation of butenes. *Appl. Catal. Gen.* *551*, 98–105.
104. Wolf, P., Logemann, M., Schörner, M., Keller, L., Haumann, M., and Wessling, M. (2019). Multi-walled carbon nanotube-based composite materials as catalyst support for water-gas shift and hydroformylation reactions. *RSC Adv.* *9*, 27732–27742.
105. Yu, S., Chie, Y., Guan, Z., Zou, Y., Li, W., and Zhang, X. (2009). Highly Regioselective Hydroformylation of Styrene and Its Derivatives Catalyzed by Rh Complex with Tetraphosphorus Ligands. *Org. Lett.* *11*, 241–244.
106. Boymans, E., Janssen, M., Müller, C., Lutz, M., and Vogt, D. (2013). Rh-catalyzed linear hydroformylation of styrene. *Dalton Trans* *42*, 137–142.
107. Sun, Q., Aguila, B., Verma, G., Liu, X., Dai, Z., Deng, F., Meng, X., Xiao, F.-S., and Ma, S. (2016). Superhydrophobicity: Constructing Homogeneous Catalysts into Superhydrophobic Porous Frameworks to Protect Them from Hydrolytic Degradation. *Chem* *1*, 628–639.
108. Cunillera, A., Blanco, C., Gual, A., Marinkovic, J.M., Garcia-Suarez, E.J., Riisager, A., Claver, C., Ruiz, A., and Godard, C. (2019). Highly Efficient Rh-catalysts Immobilised by π - π Stacking for the Asymmetric Hydroformylation of Norbornene under Continuous Flow Conditions. *ChemCatChem* *11*, 2195–2205.
109. Chen, Y., Su, P., Liu, X., Liu, H., Zhu, B., Zhang, S., and Huang, W. (2018). Titanate Nanotube-Supported Au–Rh Bimetallic Catalysts: Characterization and Their Catalytic Performances in Hydroformylation of Vinyl Acetate. *Catalysts* *8*, 420.

Figure and scheme titles and legends



Scheme 1. Reaction pathway of olefins hydroformylation and corresponding side reactions

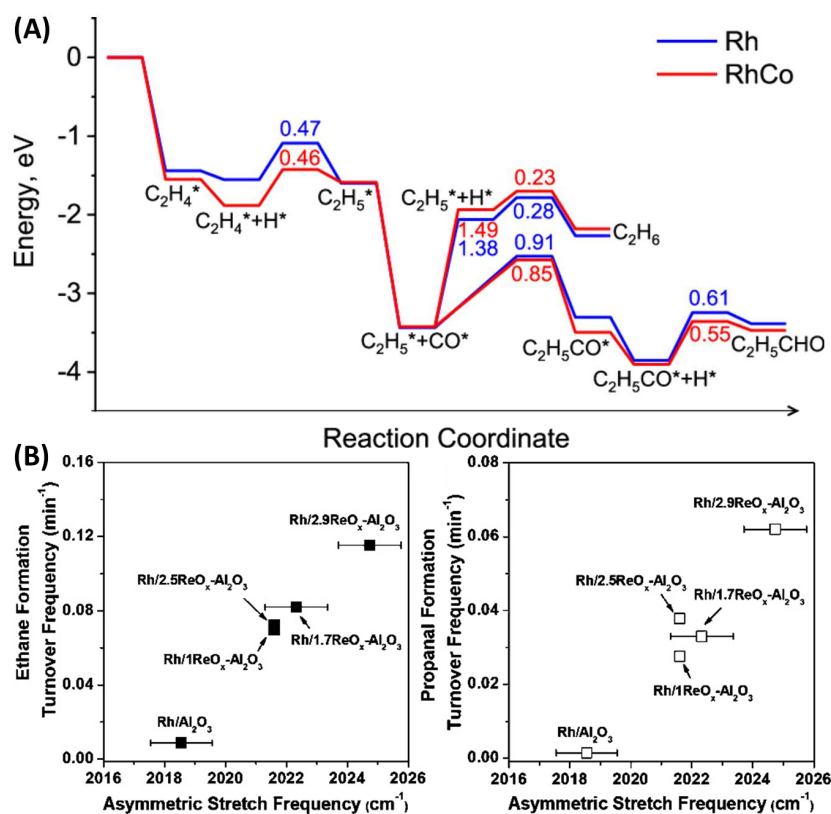


Figure 1. Reaction mechanism study of ethylene hydroformylation.

(A) Ethylene hydroformylation pathways on Rh(111) and RhCo(111) surfaces (reprinted with permission from ref ¹⁷, Copyright 2020, American Chemical Society, Washington, DC).

(B) The relationship between catalytic activity and CO stretching frequency (reprinted with permission from ref ¹⁸, Copyright 2019, American Chemical Society, Washington, DC).

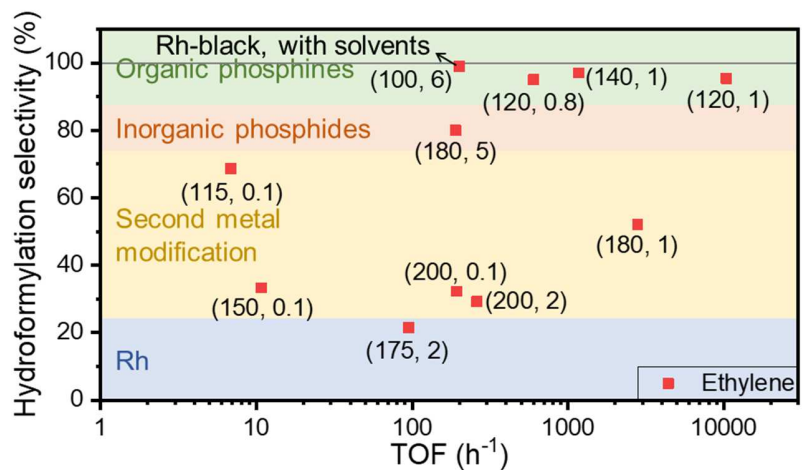


Figure 2. Summarized ethylene hydroformylation activity and chemoselectivity on different Rh-based heterogeneous catalysts. The pair of numbers in parentheses are reaction conditions, which are (temperature/°C, pressure/MPa).

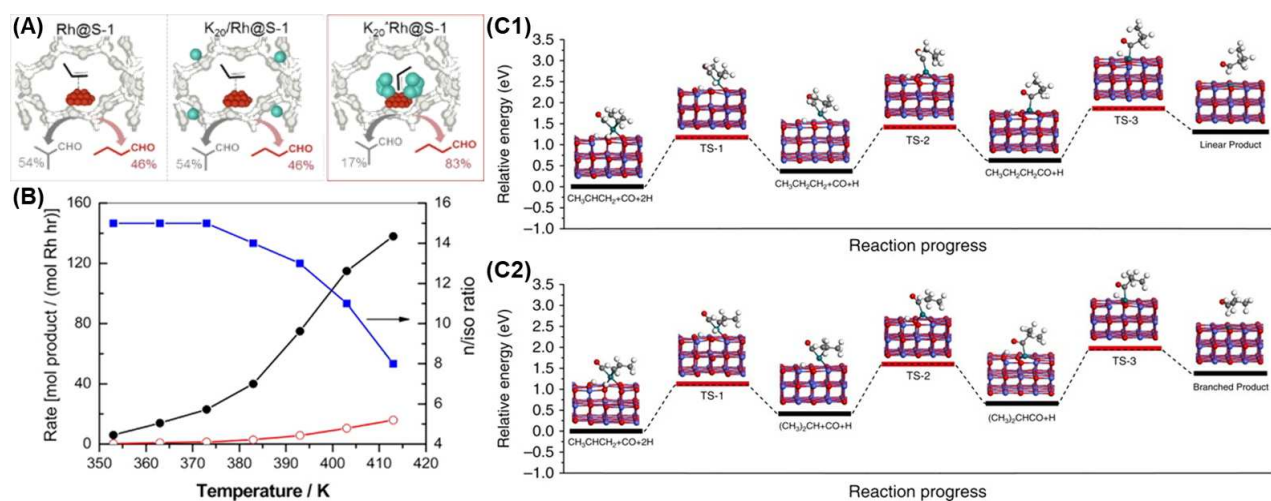


Figure 3. Modification of catalytic performance in propylene hydroformylation.

(A) Illustration of the steric hindrance for K₂₀⁺Rh@S-1 catalysts (reprinted with permission from ref ³⁰, Copyright 2020, Elsevier, Amsterdam).

(B) Effects of temperature on the regioselectivity on Rh-Xantphos/SiO₂ catalysts (reprinted with permission from ref ³¹, Copyright 2013, American Chemical Society, Washington, DC). The black and red lines represent n-butanal and i-butanal, respectively.

(C) DFT calculations of propylene hydroformylation on Rh₁/CoO catalysts to n-butanal (C1) and iso-butanol (C2) (reprinted with permission from ref ³⁵, Copyright 2016, Springer Nature, New York).

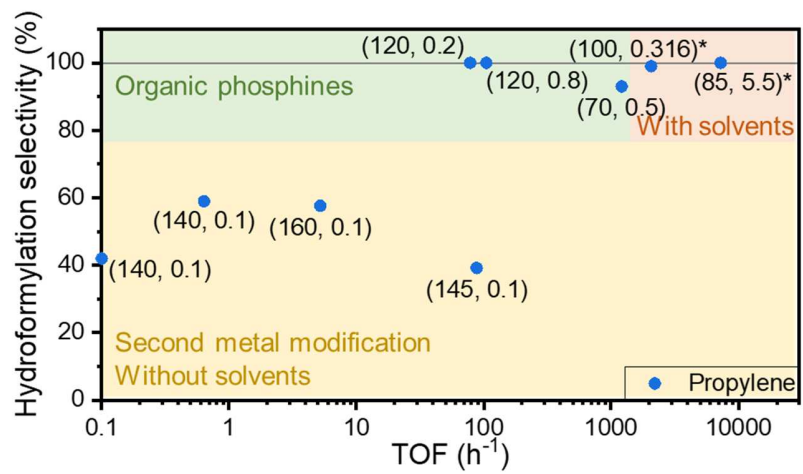


Figure 4. Summarized propylene hydroformylation activity and chemoselectivity on different Rh-based heterogeneous catalysts. The pair of numbers in parentheses are reaction conditions, which are (temperature/°C, pressure/MPa). The asterisk represents that the reaction was conducted with a solvent.

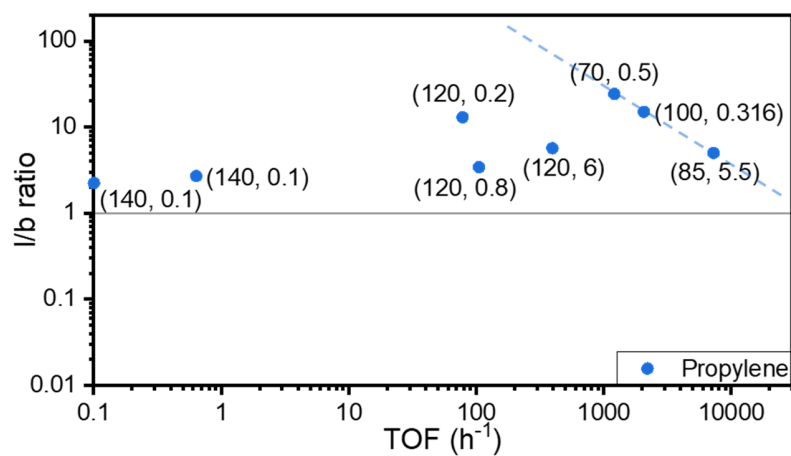


Figure 5. Summarized propylene hydroformylation activity and regioselectivity on different Rh-based heterogeneous catalysts. The pair of numbers in parentheses are reaction conditions, which are (temperature/°C, pressure/MPa).

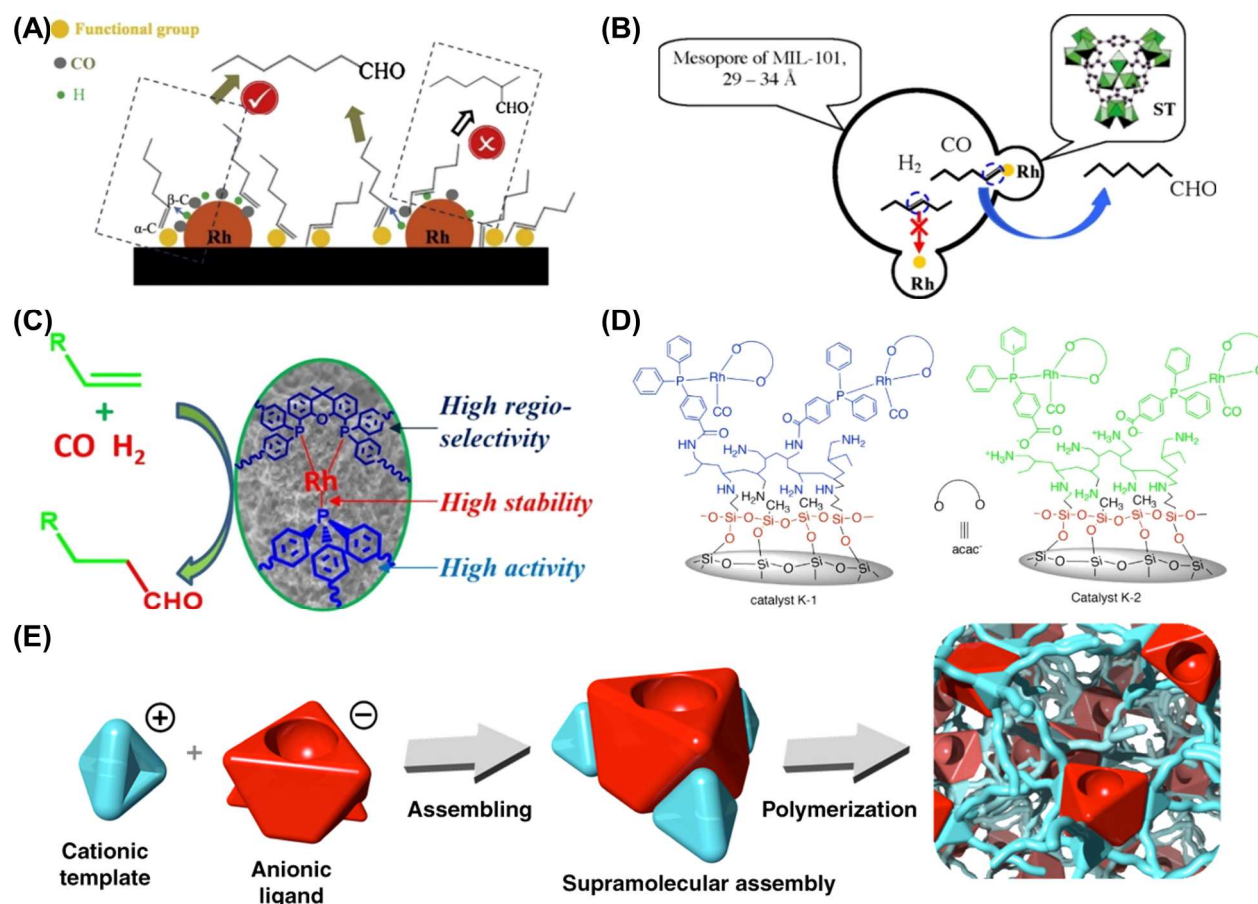


Figure 6. Catalysts designing strategies in heterogeneous hydroformylation of linear α -olefins.

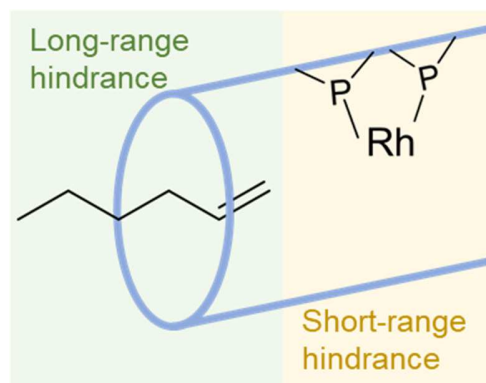
(A) Illustration of the influence of surface groups on Rh/AC-80 catalysts (reprinted with permission from ref ⁴³, Copyright 2016, Elsevier, Amsterdam).

(B) Schematic representation of the steric hindrance in Rh@MIL-101 catalysts (reprinted with permission from ref ⁴⁷, Copyright 2013, Elsevier, Amsterdam).

(C) Illustration of the ligand effects in Rh-Xantphos/POPs-PPh₃ catalysts (reprinted with permission from ref ⁵⁵, Copyright 2017, Elsevier, Amsterdam).

(D) Typical structure of Rh/silica polyamine catalysts (reprinted with permission from ref ⁵⁹, Copyright 2018, American Chemical Society, Washington, DC).

(E) Illustration of the synthesis of PSA supports (reprinted with permission from ref ⁶⁰, Copyright 2019, Springer Nature, New York).



Scheme 2. Schematic illustration of two types of steric hindrance.

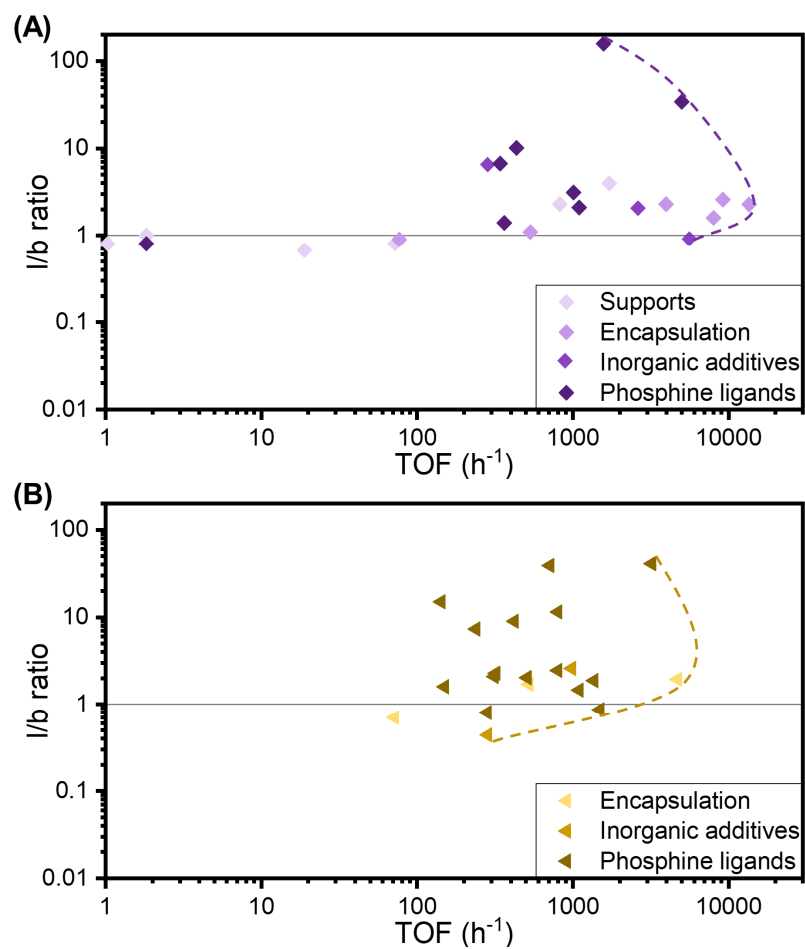


Figure 7. Summarized 1-hexene (A) and 1-octene (B) hydroformylation activity and regioselectivity on different Rh-based heterogeneous catalysts. The dashed line was the envelope curve.

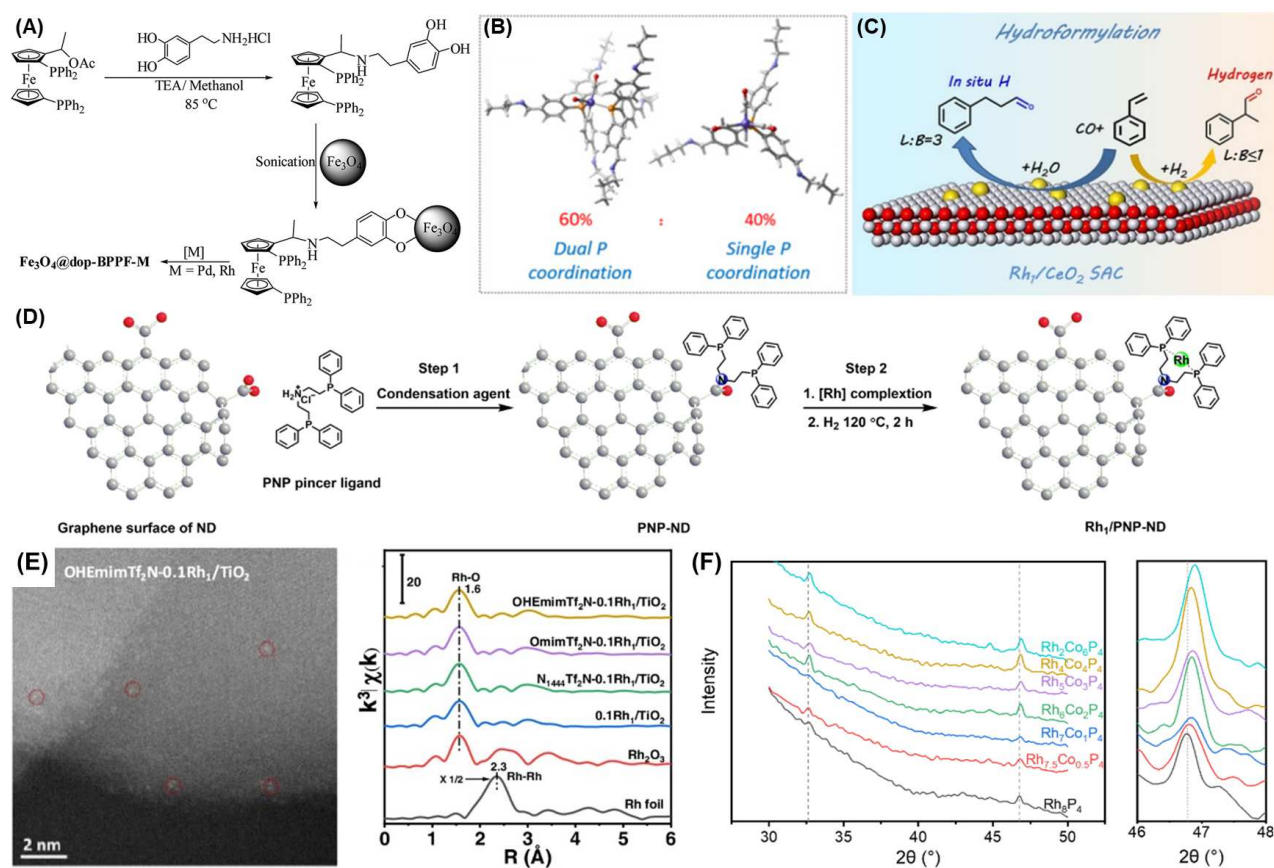


Figure 8. Catalysts design and characterization in styrene hydroformylation.

(A) Illustration of the synthesis method for Fe_3O_4 @dop-BPPF-Rh catalysts (reprinted with permission from ref ⁸⁶, Copyright 2016, Royal Society of Chemistry, London).

(B) The coordination modes of Rh/POC catalysts (reprinted with permission from ref ⁷⁶, Copyright 2021, Elsevier, Amsterdam).

(C) Illustration of the styrene hydroformylation on Rh_1/CeO_2 catalysts with in situ hydrogen (reprinted with permission from ref ⁹¹, Copyright 2020, Wiley–VCH, Weinheim, Germany).

(D) Schematic illustration of the synthesis method for $\text{Rh}_1/\text{PNP-ND}$ (reprinted with permission from ref ⁴, Copyright 2021, Springer Nature, New York).

(E) HAADF-STEM image and Fourier transform spectra of EXAFS for $\text{OHEmimTf}_2\text{N-0.1Rh}_1/\text{TiO}_2$ catalyst. (reprinted with permission from ref⁹³, Copyright 2021, Chinese Chemical Society, China)

(F) XRD patterns of $\text{Rh}_{8-x}\text{Co}_x\text{P}_4/\text{SiO}_2$ catalysts. (reprinted with permission from ref ⁹⁶, Copyright 2021, American Chemical Society, Washington, DC)

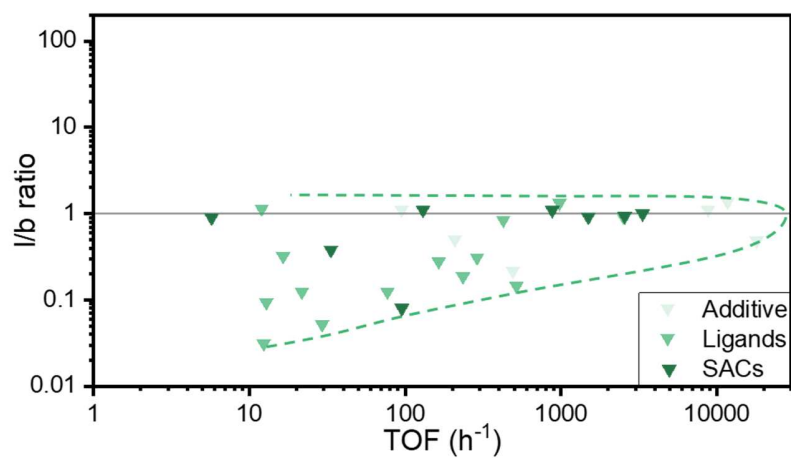


Figure 9. Summarized styrene hydroformylation activity and regioselectivity on different Rh-based heterogeneous catalysts. The dashed line was the envelope curve.

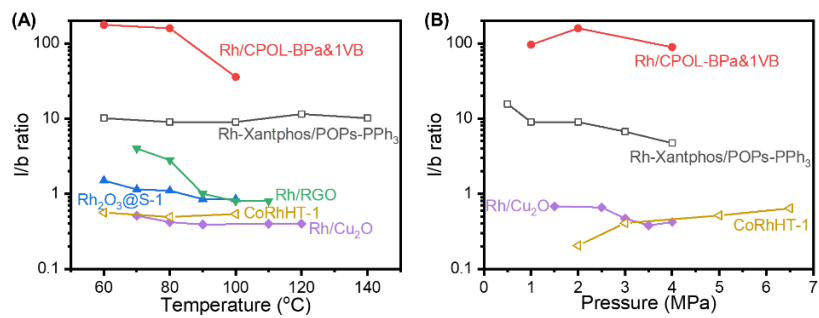


Figure 10. Effects of reaction temperature (A) and syngas pressure (B) on the regioselectivity of linear α -olefins hydroformylation. The reactants for hollow and solid symbols are 1-octene and 1-hexene, respectively. The data were obtained from ^{41,42,49,50,55,57}.

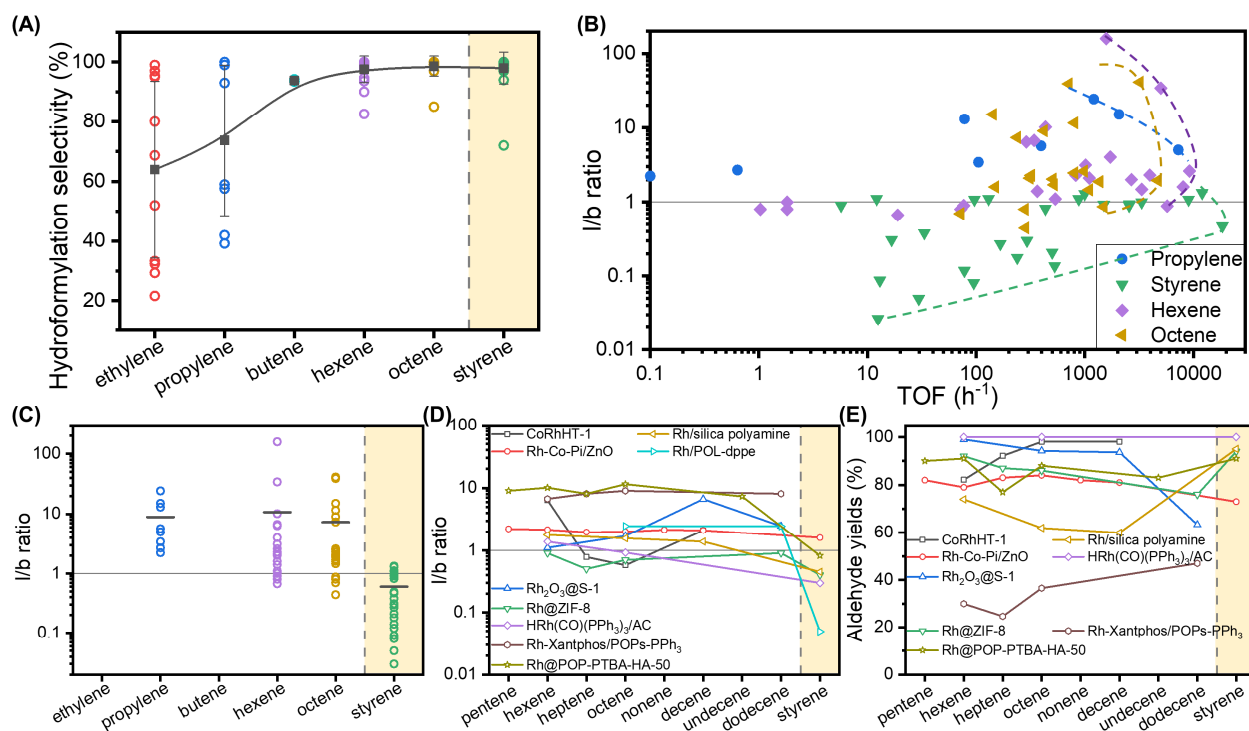


Figure 11. Summarized catalytic performance of hydroformylation reaction for different reactants.

(A) Average chemoselectivity of hydroformylation reactions with different olefin reactants. All data have been included in the above tables, except for the 1-butene hydroformylation data obtained from ref^{102–104}.

(B) Relationship between regioselectivity and catalytic activity on different catalysts. The envelop curve of each reactant was plotted in a dashed line.

(C) Average regioselectivity of hydroformylation reactions with different olefin reactants.

(D, E) Influence of reactants on the regioselectivity (D) and aldehyde yields (E) on a certain catalyst. The data were obtained from ref^{34,45,49,50,53,55,59,74,77}.

Tables and table titles and legends

Table 1. Comparison of catalysts for ethylene hydroformylation^a

Entry	Catalysts	Temperature (°C)	Pressure (MPa)	TOF (h ⁻¹)	Selectivity (%)	Ref
1	Rh/Al ₂ O ₃	175	2	94.6 ^b	21.6	12
2	Rh/MCM-41	200	0.1	156	10.1	13
3	Rh-black ^c	100	6	200	99	14
4	Rh-V/SiO ₂	115	0.1	6.84	68.7	15
5	Rh-Co/Al ₂ O ₃	200	2	260	29.3	16
6	Rh ₁ Co ₃ /MCM-41	200	0.1	192	32.3	13
7	Rh ₃ Co ₂ /SiO ₂	180	1	2790	52	17
8	Rh/2.9ReO _x -Al ₂ O ₃	150	0.1	10.8	33.3	18
9	DPPPTS-RhAl ₁ /SiO ₂	120	1	134	-	19
10	Rh-dpppe/SiO ₂	140	1	1172 ^b	97	20
11	Rh-Xantphos-SILP/NC ^d	120	0.8	600	95	21
12	Rh/POL-PPh ₃	120	1	10373	95.4	22
13	Rh ₂ P/SiO ₂ ^e	180	5	190	80	23

^a All hydroformylation reactions were conducted under gas-solid conditions and H₂/CO = 1:1, unless specified;

^b Calculated based on total Rh loading;

^c Toluene was used as the solvent;

^d H₂/CO = 2:1;

^e H₂/CO = 1:7;

Table 2. Comparison of catalysts for propylene hydroformylation^a

Entry	Catalysts	Temperature (°C)	Pressure (MPa)	TOF (h ⁻¹)	Selectivity (%) ^b	<i>l/b</i>	Ref.
1	Rh/SiO ₂	140	0.1	0.10	42	2.23	27
2	Rh-Mo/SiO ₂	145	0.1	88.1	39.2	-	28
3	Rh-V/SiO ₂	160	0.1	5.22	57.6	-	29
4	Rh-Li/SiO ₂	140	0.1	0.64	59	2.69	27
5	K ₂₀ [^] Rh@S-1 ^c	85	5.5	7238	100	5	30
6	Rh-Xantphos/SiO ₂	120	0.2	78	100	13	31
7	Rh-Xantphos-SILP/NC ^d	120	0.8	105	100	3.42	32
8	Rh/CPOL-1bp&10P	70	0.5	1209	93	24.2	33
9	Rh@POP-PTBA-HA-50 ^e	120	6	396	-	5.67	34
10	Rh ₁ /CoO ^f	100	0.316	2065	99	15	35

^a All hydroformylation reactions were conducted under gas-solid conditions and H₂/CO = 1:1, unless specified;

^b Chemoselectivity, which indicated the selectivity to oxygenates to propane;

^c Toluene was used as the solvent;

^d H₂/CO = 2:1;

^e CH₃CN was used as the solvent;

^f Isopropanol was used as the solvent;

Table 3. Comparison of catalysts for 1-hexene hydroformylation. ^a

Entry	Catalysts	Temperature (°C)	Pressure (MPa)	TOF (h ⁻¹)	Selectivity (%) ^c	Aldehydes yields (%)	<i>l/b</i>	Ref
1	Rh/SiO ₂	120	4	72 ^b	98.6	97.6	0.8	³⁹
2	Rh/nano-SiO ₂	80	4	1.82	100	77	1	⁴⁰
3	Rh/nano-ZnO	80	4	1.03	100	96	0.8	⁴⁰
4	Rh/Cu ₂ O	100	5	18.9 ^b	90	67.5	0.67	⁴¹
5	Rh/RGO ^d	70	5	1714 ^b	97.4	57.3	4	⁴²
6	Rh/AC-80 ^d	70	5	823 ^b	99.8	58.5	2.3	⁴³
7	S1/Rh/AC ^d	110	5	3955 ^b	-	-	2.3	⁴⁴
8	Rh@ZIF-8 ^e	5	5	76.7 ^b	100	92	0.9	⁴⁵
9	Rh/MOF-5	100	5	9167 ^b	82.53	44.5	2.6	⁴⁶
10	Rh@MIL-101	100	5	13496 ^b	99.4	19.4	2.29	⁴⁷
11	Rh@IRMOF-3	100	5	8000 ^b	-	40	1.6	⁴⁸
12	Rh ₂ O ₃ @S-1	80	5	533 ^b	100	99	1.1	⁴⁹
13	RhCoHT-1	100	5	289 ^b	100	83	6.36	⁵⁰
14	K ₇ ⁺ Rh@S-1	85	5	2679	100	99	2	³⁰
15	Rh-PPh ₃ /SiO ₂ ^f	100	1	1011	100	83.5	3.13	⁵¹
16	Rh-PPh ₃ /RGO ^d	90	5	1097 ^b	-	99.2	2.1	⁵²
17	HRh(CO)(PPh ₃) ₃ /AC	60	7	363 ^b	100	100	1.4	⁵³
18	HRh(CO)(TPPTS) ₃ @hydrotalcite	80	4	1.82 ^b	100	96	0.8	⁵⁴
19	Rh-Xantphos/POPs-PPh ₃	100	1	340	98	88	6.69	⁵⁵
20	Rh/POL-BPa&PPh ₃ ^d	80	2	5000	93.6	74	34.1	⁵⁶
21	Rh/CPOL-BPa&1VB ^d	80	2	1570 ^b	94.6	87.8	158	⁵⁷
22	Rh@POP-PTBA-HA-50 ^g	120	6	434	-	-	10.1	³⁴

23	Rh ₂ P@C	80	4	5727	100	92.15	0.89	⁵⁸
----	---------------------	----	---	------	-----	-------	------	---------------

^a All hydroformylation reactions were conducted in a batch reactor using toluene as the solvent and the ratio of H₂/CO = 1:1, unless specified;

^b Calculated based on total Rh loading;

^c Chemoselectivity, which indicated the selectivity to oxygenates to hexane;

^d No solvent;

^e Isopropanol was used as the solvent;

^f Cyclohexane was used as the solvent;

^g CH₃CN was used as the solvent;

Table 4. Comparison of catalysts for 1-octene hydroformylation. ^a

Entry	Catalysts	Temperature (°C)	Pressure (MPa)	TOF (h ⁻¹)	Selectivity (%) ^c	Aldehydes yields (%)	<i>l/b</i>	Ref
1	Rh@ZIF-8 ^d	5	5	71.7 ^b	100	86	0.7	45
2	Rh ₂ O ₃ @S-1	80	5	521 ^b	100	94.2	1.71	49
3	Rh@CTF ^e	80	8	4690	85	65	1.95	64
4	RhCoHT-1	100	5	284 ^b	100	92	0.44	50
5	Rh-PPh ₃ /RGO ^e	90	5	1096 ^b	-	99	1.46	52
6	Fe ₃ O ₄ @SiO ₂ -N(CH ₂ PPh ₂) ₂ Rh	80	6	320 ^b	100	82	2.28	71
7	MNP@SiO ₂ -N-Xantphos/Rh(I) ^f	80	2	2.48 ^b	100	-	-	72
8	HRh(CO)(TPPTS) ₃ @hydrotalcite	80	4	281	100	95	0.8	54
9	Rh-TPPTS@MCM-41	100	4	238	100	94	7.33	65
10	Rh/silica polyamine	80	4	150	98.99	93	1.6	59
11	Rh/silica polyamine	80	6	312	99	59.17	2.1	67
12	Rh-metallodendrimers	75	4	508	100	85	2.03	73
13	Rh/POL-PPh ₃	90	2	1491 ^b	-	91.5	0.87	68
14	Rh/POL-dppe	90	2	800	100	99.3	2.46	74
15	Rh-Xantphos/POPs-PPh ₃	100	1	420	97	87	9	55
16	Rh/POL-BPa&PPh ₃ ^c	90	2	3200	99.13	73.04	41	56
17	Rh-NiXantphos/HBPAO	75	0.48	142.5 ^b	100	95	15	75
18	Rh/PSA-Xantphos ^g	100	2	710	100	98	39	60
19	Rh/POC	100	1	1364	99.2	91.4	1.88	76
20	Rh@POP-PTBA-HA-50 ^h	120	6	801	99	84	11.5	65
21	Rh-PTA@MIL-101	70	4	980	97	60	2.6	69

- ^a All hydroformylation reactions were conducted in a batch reactor using toluene as the solvent and the ratio of H₂/CO = 1:1, unless specified;
- ^b Calculated based on total Rh loading;
- ^c Chemoselectivity, which indicated the selectivity to oxygenates to octane;
- ^d Isopropanol was used as the solvent;
- ^e No solvent;
- ^f Ethanol was used as the solvent;
- ^g Water was used as the solvent;
- ^h CH₃CN was used as the solvent;

Table 5. Comparison of catalysts for styrene hydroformylation^a

Entry	Catalysts	Temperature (°C)	Pressure (MPa)	TOF (h ⁻¹)	Selectivity (%) ^c	<i>l/b</i>	Ref
1	Rh/SiO ₂	60	5	212	99	0.49	79
2	Rh/Al ₂ O ₃	80	8	500 ^b	99.3	0.21	80
3	Rh-black	100	6	96.25 ^b	98	1.08	14
4	Rh/B-TiO ₂ -nt	80	6	18458	100	0.47	81
5	Rh/B-g-C ₃ N ₄	100	6	12000	100	1.33	82
6	Rh/S-g-C ₃ N ₄	100	6	9000	100	1.08	83
7	Rh-PPh ₃ /SiO ₂	60	5	239	99	0.18	79
8	HRh(CO)(PPh ₃) ₃ /AC	60	7	294 ^b	100	0.30	53
9	Rh-BINAP(R)/SiO ₂	60	5	13	100	0.09	84
10	Rh-BINAP(R)/SiO ₂	60	5	22	99	0.12	79
11	Rh-PAMAM/SiO ₂ -Fe ₃ O ₄	50	6.9	12.5 ^b	100	0.03	85
12	Fe ₃ O ₄ @SiO ₂ -N(CH ₂ PPh ₂) ₂ Rh	80	6	16.67 ^b	100	0.31	71
13	Fe ₃ O ₄ @dop-BPPF-Rh ^d	70	1.4	12.13 ^b	99	1.11	86
14	Rh-metallodendrimers	75	4	527	100	0.14	73
15	Rh-P-COF-1	100	2	2557	94	0.9	87
16	Rh/POL-PPh ₃	80	1	166.67 ^b	99.5	0.27	88
17	Rh/POL-dppe	50	1	29.67	100	0.05	74
18	Rh/POC	100	1	996	98.6	1.29	76
19	Rh@POP-PTBA-HA-50 ^e	120	6	434	-	0.82	34
20	Rh/BINAP polymers	80	0.2	78 ^b	-	0.12	89
21	Rh ₁ /ZnO-nw	100	1.6	3333	99	1	90
22	Rh ₁ /CeO ₂ ^f	120	3	5.72	72	0.9	91
23	Rh ₁ /CeO ₂ ^g	90	1	130	97	1.11	92

24	OHEmimTf ₂ N- 0.1Rh ₁ /TiO ₂	100	2	878	97.6	1.1	⁹³
25	Rh ₁ /Mn-MOF	80	4	33.33	100	0.38	⁹⁴
26	Rh ₁ /PNP-ND ^h	50	3	95	99	0.08	⁴
27	Rh ₂ P/SiO ₂	80	3	1496	99.5	0.92	⁹⁵
28	Rh ₇ Co ₁ P ₄ /SiO ₂	80	3	2563	98	0.94	⁹⁶
29	Rh ₇ Pd ₁ P ₄ /SiO ₂	40	6	204	99.8	0.05	⁹⁷

^a All hydroformylation reactions were conducted in a batch reactor using toluene as the solvent and the ratio of H₂/CO = 1:1, unless specified;

^b Calculated based on total Rh loading;

^c Chemoselectivity, which indicated the selectivity to oxygenates to ethylbenzene;

^d Tetrahydrofuran (THF) was used as the solvent;

^e CH₃CN was used as the solvent;

^f Dioxane was used as the solvent;

^g No solvent;

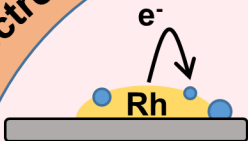
^h Mixture of toluene and water (1:1) was used as the solvent;

Table 6. Summary of challenges for different reactants and corresponding potential solutions. ^a

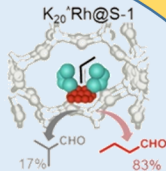
	reactants / modification strategies	activity	selectivity			stability
			chemo-	regio-	enantio-	
challenges for different reactants	ethylene	E	S	N	N	E
	propylene	E	S	S	N	E
	linear α -olefin	E	E	S	E	S
	styrene	E	E	S	E	S
potential solutions	electronic effects	S	S	E	N	E
	steric hindrance	N	N	S	S	E
	condition optimization	E	N	S	N	E

^a “E”, “S” and “N” in the table represent exist, significant and basically none, respectively.

Electronic effects



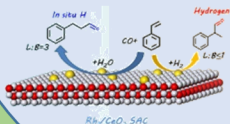
Ethylene



Propylene

Reactants

Aromatic olefins



Linear α -olefins



Steric Hindrance

Condition optimization